Special Siloxamides: Metal Movements in a Crystalline Molecular Box

Michael Veith[a]

In memoriam Prof. Dr. H.-G. Unruh

Keywords: Lithium / Solid-state structures / Phase transitions / Si ligands / Dynamics in molecular solids

Metal salts of $[R–O–SiMe_2–N–SiMe_2–O–R]^-$ and $[R–N–SiR'_2–O–SiR'_2–N–R]^{2-}$ (R = *t*Bu, Me_3Si, *t*$BuMe_2Si$, Ph; R′ = Me, Et/Me, *i*Pr; Metal = Li, Na, K, Cu, Ag) have been synthesised and analysed in the crystalline state with respect to metal movements. Almost all compounds crystallize as dimers, for example $Li_2[tBuO–SiMe_2–N–SiMe_2–OtBu]_2$ or $Li_4[tBuN–SiMe_2–O–SiMe_2–NtBu]_2$, and form different solid-state phases. Whereas the Li atoms in the first example rotate at ambient temperature perpendicular to the NN axis of the molecule, they oscillate in the second example. The movements of the lithium atoms are coupled to ligand vibrations, and can be switched on and off by temperature changes. This switching is directly linked to phase transitions, that can be first order or second order. The other metallic atoms show no important dynamics, although phase transitions have also been found for these compounds.

Introduction

In the last ten years we have become aware of the fact that special amides of metallic elements (lithium amides being the most prominent representatives) show fluxional behaviour, mostly when dissolved in non-coordinating organic solvents.[1–3] The phenomenon is known for many amides of the main-group and transition-group metals, and the dynamics of these compounds can easily be followed by temperature-dependent NMR spectroscopy.[4] On analysing the molecules in more detail we found, compared to all other elements, the small lithium atoms in the amides have the largest amplitudes of movement, and that these amplitudes and the trajectories of the movements can be influenced by the composition of the amides. A spectacular example is the mixed metal amide $LiIn[(Me_3SiN)_2SiMe_2]_2$:[5] In this molecule the indium atom with a formal charge +3 is coordinated by the four nitrogen atoms, forming an indium-centred N_4 bisphenoid (elongated tetrahedron), pushing the lithium atom, with a formal charge +1, to the surface of the N_4 polyhedron. Because the lithium atom in this molecule is less tightly bound, it occupies several similar coordination sites, and in solution it rotates, over a certain time period, around the indium-centred N_4 core. The movement of the lithium atom can be determined experimentally, either by temperature-dependent ^{7}Li-, ^{13}C-, ^{1}H-, ^{29}Si-NMR spectroscopy, or by theoretical calculations.[6]

We were interested in finding out if similar lithium movements could be observed in crystalline solids. As the constraints of the crystal packing on the molecules and the intermolecular forces seemed to make such an attempt quite fruitless, we developed a concept which had two main ideas. The first idea was to use molecules which had a globular outer hydrogen shell to minimise the intermolecular van der Waals interactions. The second idea was to incorporate coordination holes in the molecular skeleton, so as to facilit-

[a] Institut für Anorganische Chemie, Universität des Saarlandes
Postfach 151150, 66041 Saarbrücken, Germany
Fax: (internat.) + 49-(0)681/302-3995
E-mail: veith@rz.uni-sb.de

Michael Veith was born in 1944 in Goerlitz, Germany. He studied chemistry at the University of Munich, where he received his Diplom-Chemiker degree in 1969. Continuing work with Prof. N. Wiberg, he received his doctoral degree in 1971. He then moved to the University of Karlsruhe, where he started his postdoctoral work with Prof. H. Bärnighausen. In 1977 he completed his Habilitation in Inorganic Chemistry. Until the end of 1978 he was Privat-Dozent at the University of Karlsruhe. In 1979 he moved to the Technische Universität Braunschweig as a Professor of Inorganic Chemistry. In 1984 he moved to the University of Saarland (Saarbrücken) and became Full Professor. Since 1984 he has been in Saarbrücken despite several offers from other universities. He has received several awards, inter alia Leibniz-Preis, 1991. In 1981, he stayed as a visiting professor at the University of Bordeaux I (France) and in 1987 at the University of Utah (Salt Lake City, USA), in 1991 at the University Paul Sabatier (Toulouse, France), and in 1993 at the University Sophia Antipolis (Nice, France). His main interests are in the field of synthetic and structural chemistry, focusing on molecular compounds containing metal elements.

 © WILEY-VCH Verlag GmbH, D-69451 Weinheim, 2000 1434–1948/00/0909–1883 $ 17.50+.50/0

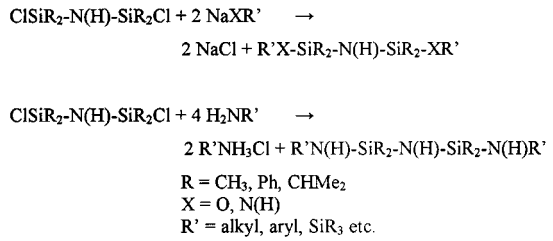

Scheme 1

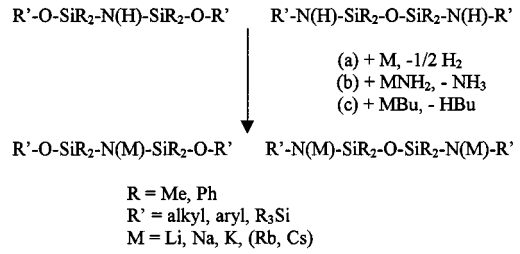

Scheme 3

ate metal hops from an occupied non-metal coordination sphere to an unoccupied one.

The following compilation, which can be seen as an advanced report with a review-like character, is a summary of our actual knowledge on the motion of monovalent metal atoms in the molecular crystals of special metal amides. We would like to describe these dynamics as "lithium motion (or tunnelling) in a molecular box". The compounds we have investigated belong either to the series $[R'-O-SiR_2-N-SiR_2-O-R']_2M_2$ or to the series $[R'-N-SiR_2-O-SiR_2-N-R']_2M_4$ (R' = substituent, M = monovalent metal, R = organic group). While these experiments were being conducted, several papers appeared on either lithium movements[7] or the use of the amido ligands specified above as assembling tools for different metallic elements.[8,9]

Syntheses

The most valuable precursor compounds for the siloxamines $R'-O-SiR_2-N(H)-SiR_2-O-R'$ and $R'-N(H)-SiR_2-O-SiR_2-N(H)-R'$ are either the bis(silyl)amine $ClSiR_2-N(H)-SiR_2Cl$[10] or the disiloxane $ClSiR_2-O-SiR_2Cl$.[11] As shown in Scheme 1 and Scheme 2, the chlorine atoms of chlorosilylamines and chlorosiloxanes can be easily substituted by amido or alkoxo groups in a straightforward way.[4]

The transformation of these siloxamines into siloxamides can be achieved by a redox/metal route (a), a transamidation (b), or by organometallic compounds (c). All three possible reactions are shown in Scheme 3.[4]

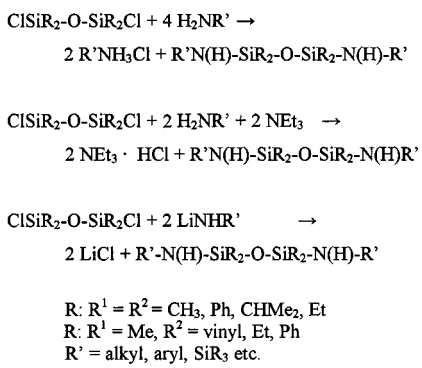

Scheme 2

The reactions are very dependent on the alkali element and the substituent R'. The higher the electropositive character of the R' group (e.g. CMe_3 vs. $SiMe_3$) the more preferable the replacement of the hydrogen atom by the alkali metal atom. Similarly, more electropositive alkali elements will normally more easily replace the hydrogen atom attached to the nitrogen atom. Finally, the organometallic route (3c) is more generally applicable, and gives the best yields for the metal amides.

The solvents for these reactions should be completely dry and noncoordinating, such as pentane, hexane, and toluene, since adducts of the solvent with the alkali metals have to be avoided. The more electropositive alkali elements K, Rb, and Cs do not always give pure compounds, and are introduced into the amine $R'-N(H)-SiR_2-O-SiR_2-N(H)-R'$ less readily than lithium or sodium. This feature is exemplified by the reaction of tBu$-N(H)-SiMe_2-O-SiMe_2-N(H)-t$Bu with butyllithium, -sodium,[12] and -potassium.[13] While the pure dilithium and disodium derivatives can be obtained in the first two cases, for potassium only a mixed metal derivative is obtained, which incorporates lithium as well as potassium (Scheme 4).

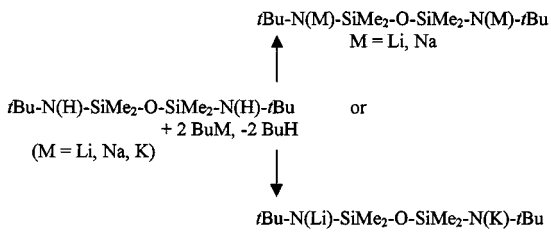

Scheme 4

The explanation for this unexpected reaction is the incomplete transformation of BuLi to BuK, when butyllithium is treated with potassium *tert*-butoxide prior to the reaction with the amine. Perhaps the "incomplete" BuK formation could be avoided by using potassium *tert*-pentoxide instead of potassium *tert*-butoxide.[14] Interestingly, the mixed metal derivative is isolated in high yields, which suggests that both metal atoms may be especially well accommodated in the molecule. As a matter of fact, tBu$-N(Li)-SiMe_2-O-SiMe_2-N(K)-t$Bu is dimeric, as are most of the other derivatives, and the two alkali elements have very different coordination spheres (see below for more details of the structure). This structure cannot be achieved in a pure dilithium or dipotassium derivative.

The alkali metal derivatives shown in Scheme 3 can be transformed into other metal derivatives, using metal halides. Especially monovalent transition metals were of interest for our general study. The copper(I) and silver(I) derivatives of the $[t\mathrm{Bu-N-SiMe_2-O-SiMe_2-N-}t\mathrm{Bu}]^{2-}$ dianion have been obtained in high yields using this route (Scheme 5).

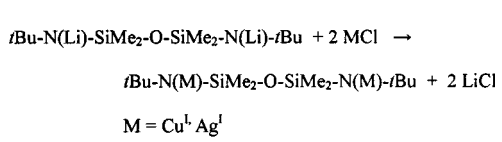

Scheme 5

The siloxamides of most alkali elements as well as the Cu^I and Ag^I derivatives that have been synthesised and characterised by our group are listed in Table 1.[15–19] Most of these compounds are dimeric in solution and in the crystalline state. So far there is only one exception to this rule: The compound $t\mathrm{Bu-N(Li)-Si}(i\mathrm{Pr})_2\mathrm{-O-Si}(i\mathrm{Pr})_2\mathrm{-N(Li)-}t\mathrm{Bu}$ is monomeric in solution as well as in the crystal (see also below).

The solution NMR spectra of the two families $[\mathrm{R'OSiR_2-N(M)-SiR_2OR'}]_2$ and $[\mathrm{R'N(M)-SiR_2-O-SiR_2-N(M)R'}]_2$ at room temperature are very simple, as all substituents R and R′ (^{1}H, ^{13}C NMR) and silicon atoms of the siloxamine backbone (^{29}Si) give resonances for only one species, the other groups being symmetry-related. This is in sharp contrast to the generally less symmetrical molecules in the crystalline solid. Consequently, many of these molecules show bond fluctuations in solution that are connected with metal movements or displacements. As we wanted to concentrate on such dynamics in the solid state, we will not discuss the solution phenomenon here in more detail.

Table 1. Siloxamides of the two different backbones O−Si−N−Si−O (**A**) and N−Si−O−Si−N (**B**)

	A
Z	$\mathrm{R_3C-O-SiMe_2-N-SiMe_2-O-CR_3}$, R = $\mathrm{CH_3}$
	Li_2Z_2, Na_2Z_2, K_2Z_2, Rb_2Z_2
Z′	$\mathrm{Ph-O-SiMe_2-N-SiMe_2-O-Ph}$
	$Li_2Z'_2$
Z″	$\mathrm{Me_3Si-O-SiMe_2-N-SiMe_2-O-SiMe_3}$
	$Li_2Z''_2$
	B
X	$\mathrm{R_3C-N-SiR_2-O-SiR_2-N-CR_3}$, R = $\mathrm{CH_3}$
	Li_4X_2, Na_4X_2, $Li_2K_2X_2$, Cu_4X_2, Ag_4X_2
X′	$\mathrm{R_3C-N-SiRR'-O-SiRR'-N-CR_3}$, R = $\mathrm{CH_3}$, R′ = $\mathrm{CH{=}CH_2}$
	$Li_4X'_2$
X^I	$\mathrm{R_3C-N-SiRR'-O-SiRR'-N-CR_3}$, R = $\mathrm{CH_3}$, R′ = $\mathrm{CH_2-CH_3}$
	$Li_4X^I_2$, $Na_4X^I_2$
X^{II}	$\mathrm{R_3C-N-SiR'_2-O-SiR'_2-N-CR_3}$, R = $\mathrm{CH_3}$, R′ = $\mathrm{CH(CH_3)_2}$
	Li_2X^{II}
L	$\mathrm{R_3Si-N-SiR_2-O-SiR_2-N-SiR_3}$, R = $\mathrm{CH_3}$
	Li_4L_2, Na_4L_2
L′	$\mathrm{R_2R'Si-N-SiR_2-O-SiR_2-N-SiR'R_2}$, R = $\mathrm{CH_3}$, R′ = $\mathrm{C(CH_3)_3}$
	$Li_4L'_2$

Structural Characterisations of the Siloxamides

As the goal of our investigations was to study movements of atoms or molecular entities within a molecule, we have used different structural analysis techniques like X-ray diffraction on single crystals or powders, broad-line or MAS (magic angle spinning) NMR, differential thermal analysis (DTA), and Raman spectroscopy on single crystals. All these techniques have been used in the temperature-dependent mode, generally in the range between 120 and 350 K, using liquid nitrogen as a cooling agent or as a heated gas flow. Light microscopy on single crystals using polarised or cross-polarised light in the same temperature range was also employed. To verify our assumptions, which are based on our experimental results, we have tentatively used molecular dynamics calculations with mostly standard parameters.[20]

It became more and more evident from our experiments that phase transitions are connected with movements in the solid state. To avoid complications such as twinning, arising from symmetry reductions in single crystals, we have systematically also done X-ray diffraction experiments from phases, which have been grown as single crystals in the appropriate temperature range. Furthermore, we collected most of the X-ray diffraction data on a two-dimensional screen (IPDS system of Stoe, Darmstadt) in small angle steps, in order to obtain information about the whole reciprocal space.

High symmetries corresponding to unusual space groups for molecules can come either from dynamics or from severe static disorder of the constituent atoms. In this respect, the combination of X-ray diffraction techniques with solid-state NMR techniques is an excellent tool for deciding between these two possibilities.

Our findings are presented in several chapters which are linked in some logical sense (to follow and to verify our assumptions they have to be read together).

Rotation of Lithium Atoms within a Molecule: Siloxamides with the Skeleton O−Si−N−Si−O

The compound $\mathrm{Li_2}[t\mathrm{Bu-O-SiMe_2-N-SiMe_2-O}t\mathrm{Bu}]_2$, designated in the following sections as **Li_2Z_2**, forms three different crystalline phases in the solid state.[15] At temperatures < 285 K a monoclinic phase is found, space group $P2_1/n$ with $Z = 4$. The space group with the number of molecules per cell is consistent with a close packing of organic molecules using the well-established principles of Kitaigorodskii.[21] A drawing of the molecule at 220 K is shown in Figure 1.

There are two main observations: The two "anionic" ligands within the molecule are opposite to each other in a cross-like manner, and are linked by two lithium "cations", which are bisphenoidally coordinated by two nitrogen and two oxygen atoms ("elongated" tetrahedron). The zigzag chain C−O−Si−N−Si−O−C is a little bit twisted, but the deviation from the plane is not intriguing, as the largest dihedral angle of two adjacent angles (O−Si−N−Si and Si−N−Si−O) is around 20°. As a consequence of these

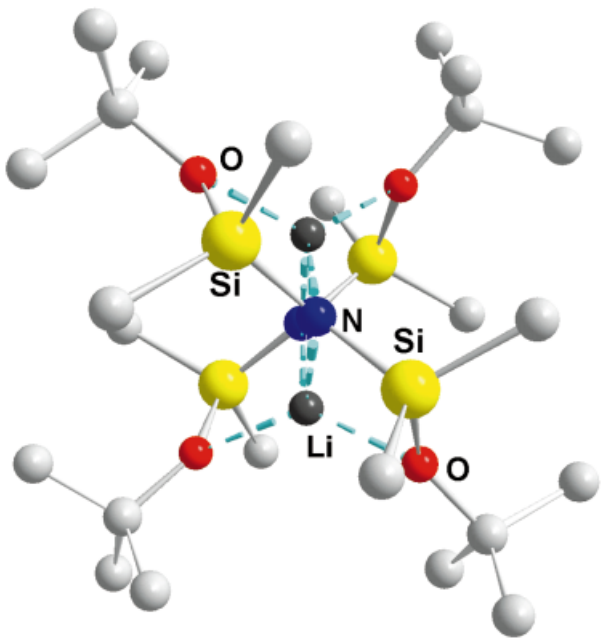

Figure 1. Spectroscopic view of $Li_2[tBu-O-SiMe_2-N-SiMe_2-OtBu]_2$, $\mathbf{Li_2Z_2}$, in the monoclinic low-temperature phase (220 K), as obtained from X-ray diffraction analysis; view almost parallel to the NN axis of the molecule; for some distances and angles refer to Table 2

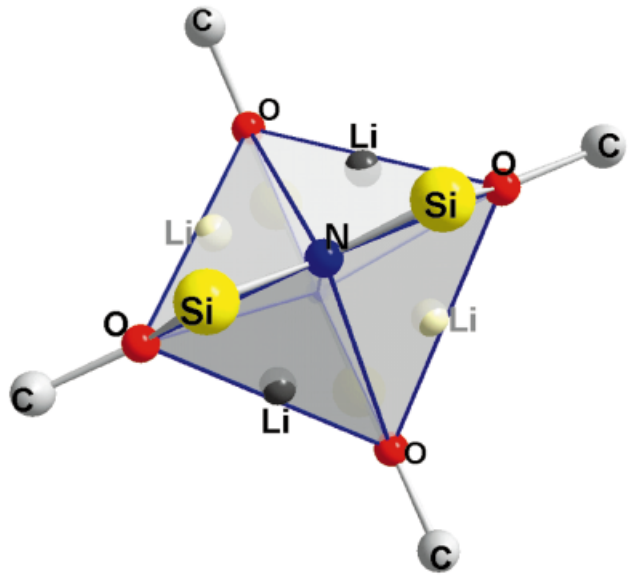

Figure 2. Inner part of the atomic skeleton of $Li_2[tBu-O-SiMe_2-N-SiMe_2-O-tBu]_2$ in the tetragonal phase (295 K), as obtained from X-ray diffraction analysis; the coordination polyhedra are drawn; each of the four N_2O_2 holes is occupied with Li/2 (see text)

mutual orientations of the ligands, two other bisphenoidal O_2N_2 coordination spheres are formed, that are unoccupied. In exact correspondence to the X-ray structure analysis of the monoclinic phase of $\mathbf{Li_2Z_2}$, the ^{13}C-MAS NMR spectrum of the crystalline powder is quite complex, showing a multiplet of signals in the H_3C-Si region, that after deconvolution can be shown to be a superposition of eight equal signals due to eight different carbon atoms bonded to the four non-equivalent silicon atoms. Due to quadrupolar coupling of the coordinated nitrogen atoms, the ^{29}Si-MAS NMR resonances are broadened and structured, but it can again be shown that more than two resonances from silicon atoms are present in the spectrum (X-ray crystallography shows that four different silicon atoms are present in the unit cell).

When $\mathbf{Li_2Z_2}$ is allowed to warm up to room temperature (295 K), a new phase is found that is tetragonal (space group $P4_2/nmc$ with $Z = 2$). Whereas $\mathbf{Li_2Z_2}$, in the monoclinic phase lacks symmetry [point symmetry $C_1(1)$], in the tetragonal phase the point symmetry is $D_{2d}(\bar{4}2m)$. The phase transition is reversible with a small hysteresis and an endothermic heat ($\Delta H = +0.45$ kJ/mol). The refinement of the X-ray structure of $\mathbf{Li_2Z_2}$ in $P4_2/nmc$ has only been possible with relatively high anisotropic displacement factors for Si, O, and N, and split atoms for most of the carbon atoms, the primary carbon atoms of the *tert*-butyl group being disordered around the O−C axis. The most striking feature is nevertheless the splitting of the two lithium atoms that occupy, with half of their electron count, the four coordination holes formed by the four oxygen and two nitrogen atoms (see Figure 2).

Again all the findings in the X-ray diffraction experiments are paralleled in the solid-state NMR spectra. The multiplet of the silyl carbon atoms of the monoclinic phase of $\mathbf{Li_2Z_2}$ after transition to the tetragonal phase degenerates to a single resonance line (^{13}C-MAS NMR). All carbon atoms of the dimethylsilyl groups become equivalent, consistent with the $D_{2d}(\bar{4}2m)$ point symmetry of the molecule. The silicon multiplet (^{29}Si-MAS NMR) also becomes a singlet after phase transition (not considering the quadrupolar splitting by N). These two experiments unambiguously show that the higher point symmetries found in the X-ray structure analysis are due to *dynamic* and not *static* disorder.

From the X-ray structure analysis of $\mathbf{Li_2Z_2}$ (considering temperature factors and split atom positions) we found that the lithium atoms (or in an ionic model: cations) clearly move to a larger extent than all other atoms of the molecule. The lithium movement can be followed directly by use of ^{6}Li- and ^{7}Li-NMR experiments applying the broad-line mode and the MAS mode. How can we describe this movement in the tetragonal phase? The most simple explanation would be that the lithium atoms (ions) are jumping from the occupied bisphenoidal O_2N_2 holes into the unoccupied ones. An approximate calculation (molecular mechanics in vacuo) of the barrier for this process using the parameters from the X-ray structure determinations of the monoclinic and tetragonal phase show that this jumping should be quite unfavourable, with activation energies around 60 kJ/mol (the lithium atoms are assumed to be positively charged).[20] Things become quite different, when the simultaneous movement of the ligands is included in the calculations: Now the barriers are drastically lowered and the activation energy is estimated to approximately 10 kJ/mol at 20°C.[20]

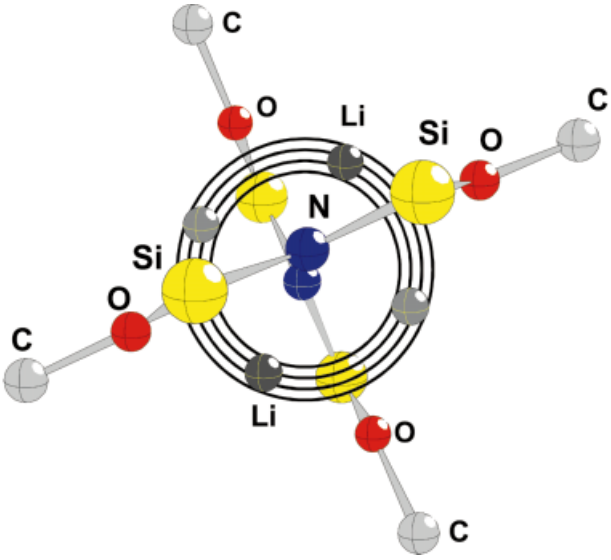

Figure 3. Sketch of the intramolecular lithium movements in the tetragonal phase of $Li_2[tBu-O-SiMe_2-N-SiMe_2-OtBu]_2$; the four split atom positions of lithium are shown; it should be noted that the lithium movements are accompanied by atom vibrations of the ligands (see also Figure 2)

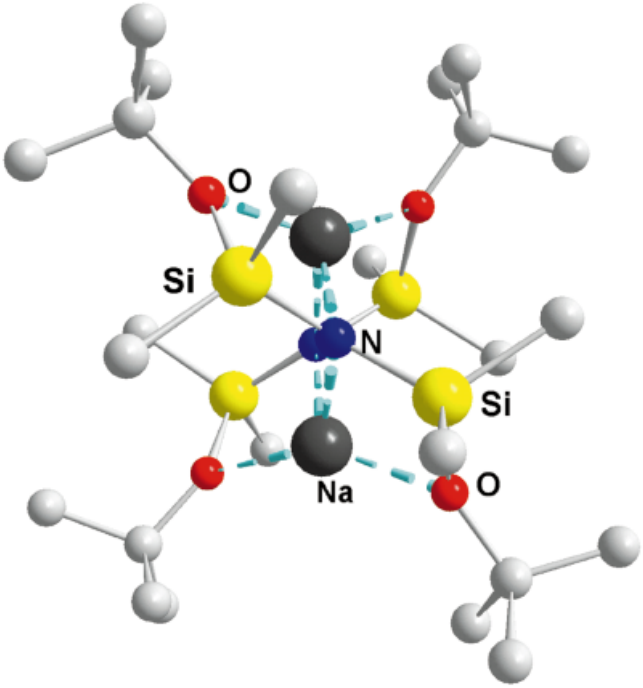

Figure 4. One of the two molecules [crystal point symmetry $C_2(2)$] present in the monoclinic phase of $Na_2[tBu-O-SiMe_2-N-SiMe_2-OtBu]_2$ (**Na_2Z_2**); for some distances and angles refer to Table 2; the view of the molecule is taken almost parallel to the NN axis of the molecule

In a crystalline solid, the amplitudes of movements of the atoms are nevertheless limited. On the other hand, the molecular shape and packing of **Li_2Z_2** is quite special; as can be deduced from two phenomena: The methyl groups of the *tert*-butyl moieties are turning around their O−C axes (as can be derived from X-ray structure analysis and ^{13}C-MAS NMR). The other phenomenon is found at temperatures > 400 K, where a second phase transition occurs and **Li_2Z_2** crystallises in a cubic face-centred lattice. This high-temperature phase is typical of a "plastic crystal phase", with molecules "tumbling" around their centres of gravity. Such "plastic crystal phases" are known for molecules that are either very globular in shape or possess weak intermolecular van der Waals interactions.[21]

Considering these two pieces of information, and the geometrical constraint of the O_2N_2 holes within the molecule, the movements of the lithium atoms can be described as follows: the lithium atoms, which to a first approximation can be assumed to be charged +1, are turning around the NN axis of the molecule, jumping from one O_2N_2 hole to the neighbouring hole. As the distances between two neighbouring N_2O_2 holes are small (the centres are 1.45 Å apart from one another in the tetragonal phase), the lithium atoms have to jump (or to turn) *simultaneously* to reduce the Li−Li repulsive forces. In Figure 3 the model of this rotation is sketched. Two models for the lowering of the activation energy can be discussed: One is using the tunnelling approach, assuming the lithium cations to be quite small. The other is considering, in addition to the jumping of the Li ions, a simultaneous high vibrational freedom of the ligands, which in the free molecule would lower the activation energy considerably (vide supra). Anyhow, the high displacements of vibration of the ligands have to be coupled to the lithium movements.

The two phase transitions in the solid **Li_2Z_2** are of first order, as can be deduced from the sharp changes of the cell parameters or of the spectroscopic properties (NMR) at the transition points. An elegant way to follow the phase transitions is Raman spectroscopy on single crystals: these methods show clearly that the two transitions occur instantaneously without softening of any vibrational mode.[22] Again this agrees with first-order phase transitions. Nevertheless, the hysteresis of the phase transition between the monoclinic and tetragonal phase is quite small, and the "lithium rotations" can be switched on and off, just by changing the temperature. Interestingly, this can even be made with a single crystal, which does not fall to pieces, as the volume of the cells is approximately unchanged (taking the double tetragonal cell). $P4_2/nmc$ and $P2_1/n$ are symmetry-related, but not in a direct super group/sub group relationship.[15]

We were very curious to know how an exchange of the lithium atom by sodium would influence the phase transitions, especially the movements in the molecules within the crystal lattice. Sodium has a larger radius compared to lithium [$r(Li^+) \approx 0.76$ Å; $r(Na^+) \approx 1.02$ Å], and its mass is approximately three times that of lithium.[23] Under these circumstances, a tunnelling of sodium cations seemed to be very improbable. The molecule $Na_2[tBuO-SiMe_2-N-SiMe_2-OtBu]_2$, [**$Na_2Z_2$**], crystallises at temperatures below 250 K in an unknown lattice, and between 250 K and 350 K in the monoclinic space group $P2/n$ with $Z = 4$, very differently from **Li_2Z_2**. In the room-temperature phase there are two independent molecules in the unit cell, both situated on two-fold axes of the space group. In Figure 4 the

Table 2. Comparison of M−N, M−O, MM, NN, OO, and NO distances [Å] and O−M−O angles [°] in the two molecules $M_2[tBuO-SiMe_2-N-SiMe_2-OtBu]_2$, $\mathbf{Li_2Z_2}$ (230 K) and $\mathbf{Na_2Z_2}$ (290 K); mean values, monoclinic phases

	M−N	M−O	NN	OO[a]	NO	OO[b]	O−M−O	MM
$\mathbf{Li_2Z_2}$	2.075(8)	1.990(8)	3.333(7)	3.711(7)	3.134(7)	4.504(7)	136.2(1)	2.473(9)
$\mathbf{Na_2Z_2}$	2.433(5)	2.282(5)	3.842(7)	4.456(7)	3.452(7)	5.001(7)	155.0(1)	2.972(4)
Δ [$\mathbf{Na_2Z_2}$ − $\mathbf{Li_2Z_2}$]	0.358	0.292	0.509	0.745	0.318	0.497	18.8	0.499

[a] N_2O_2 hole occupied by M. − [b] Unoccupied N_2O_2 hole.

molecular structure of one $\mathbf{Na_2Z_2}$ species is drawn; the two molecules differ from each other by the degree of disorder of the *tert*-butyl groups around the O−C axis. The molecules approach the D_2(222) point symmetry very closely, as may also be deduced from inspection of Figure 4.

Two major differences may be seen by comparing the monoclinic phases of $\mathbf{Na_2Z_2}$ with $\mathbf{Li_2Z_2}$. One discrepancy between the two compounds is easily recognised by closer inspection: The zigzag O−Si−N−Si−O chain in $\mathbf{Na_2Z_2}$ deviates more from an equiplanar arrangement (the mean O−SiSi−O dihedral angle is 73°) than in $\mathbf{Li_2Z_2}$ (45°). Consequently, looking down the NN axis of the molecule, the four silicon atoms with the nitrogen atoms are less perpendicularly oriented ($\mathbf{Na_2Z_2}$: Si−NN−Si = 116°) than in $\mathbf{Li_2Z_2}$ (Si−NN−Si = 100°). The second difference can be seen in the Na−O and Na−N distances in $\mathbf{Na_2Z_2}$. They are longer than the corresponding Li−O and Li−N distances in $\mathbf{Li_2Z_2}$ (monoclinic phases), and the sodium atoms (ions) are located far away of the centres of N_2O_2 holes (see also Δ values in Table 2). The lithium atoms are better accommodated in the O_2N_2 holes than the sodium atoms, which can for example be deduced from the O−Li−O angle (136°) and the corresponding angle in $\mathbf{Na_2Z_2}$ O−Na−O (155°). The large value of the latter shows that it tends towards linearity. The solid-state NMR spectra of $\mathbf{Na_2Z_2}$ agree with the structures found from X-ray diffraction. In the Si−C region of the ^{13}C-MAS NMR spectrum, at least four different peaks can be seen, that seem to come from the superposition of eight different resonances (four for each molecule, both of which have C_2 crystal symmetry). The four resonances are in accordance with the almost perfect D_2 symmetry of the molecules.

When crystals of $\mathbf{Na_2Z_2}$ are allowed to warm above 350 K, a phase transition can be observed by DTA with an endothermic $\Delta H \approx 5$ kJ/mol at 113°C. This phase transition can also be followed by temperature-dependent ^{13}C-MAS NMR (Figure 5). The crystal symmetry becomes orthorhombic, with a doubling of the volume of the monoclinic cell. An analysis of systematic absences in the X-ray powder diffraction experiment leads to a face-centred lattice (*Fd*2*d* or *Fddd*) with $Z = 8$, which has two consequences: All molecules in the unit cell are equal, and the point symmetry should be at least C_2, and is more likely D_2. In Figure 5 the two ^{13}C-MAS NMR spectra of the monoclinic and orthorhombic phase in the Me−Si region are shown for comparison.

As can be seen in the high temperature phase there are still *two* ^{13}C-NMR resonances for the CH_3−Si groups. This

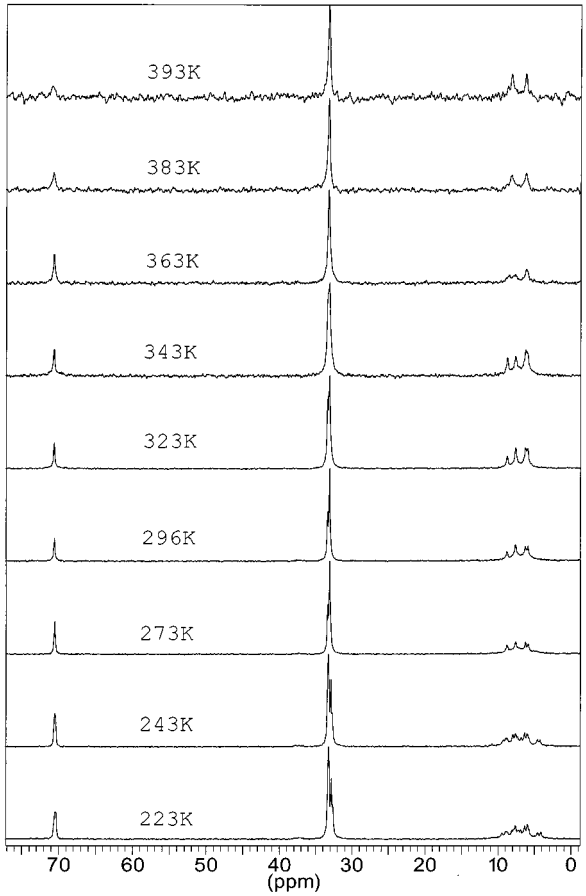

Figure 5. ^{13}C-MAS NMR spectra of $Na_2[tBu-O-SiMe_2-N-SiMe_2-OtBu]_2$ ($\mathbf{Na_2Z_2}$) between 190 and 380 K

agrees with either D_2 or C_2 point symmetry of the unique molecule present in the asymmetric unit. It also shows nicely, that *no sodium jumping* is occurring in this phase: If sodium jumping occurred then there should be a singlet for the 8 methyl groups attached to the silicon atoms. What might be the reason for the phase transition of $\mathbf{Na_2Z_2}$ at 400 K? The ^{13}C-NMR spectra indicate that most of the *tert*-butyl groups rotate in the high-temperature phase. At the same time, because of the new freedom of motion, the molecules can adopt higher point symmetries. This phase transition is another example of a temperature-dependent gain of motional freedom which we have already found for $Me_2Si(NtBu)_2Sn(NtBu)_2SiMe_2$ many years ago![24] The overall higher energy at 400 K cannot be used for sodium motions presumably because the trajectories for the heavy sodium atoms in $\mathbf{Na_2Z_2}$ are much longer than those of li-

thium atoms in $\mathbf{Li_2Z_2}$ and the sodium atom is larger and heavier than lithium (see before).

The high-temperature orthorhombic phase of $\mathbf{Na_2Z_2}$ can already be deduced from the monoclinic room-temperature phase as the cell dimensions may easily transformed to orthorhombic axes [a = 20.86(1), b = 10.303(8), c = 21.17(1) Å, β = 119.50(5)°]. The unusual presence of two different molecules of point symmetry C_2 in the $P2/n$ space group, on the other hand may be rationalised by a further low-temperature phase, the room-temperature structure being only a transient phase. Indeed, by cooling the polycrystalline sample, a further low-temperature phase was identified from ^{13}C-MAS NMR experiment (transition point: at 260 K). In this spectrum below 260 K, the C−Si region is split into many signals (at least 13−14 can be distinguished) which shows that in this low-temperature phase there are still two molecules in the asymmetric unit, but the point symmetry of these molecules is now reduced to C_1 (theoretically 16 signals should appear in the spectrum, Figure 5).

So far it seems that with the rise in temperature the $\mathbf{Na_2Z_2}$ compound is steadily gaining point symmetry showing two phase transitions: 260 K: 2 independent molecules with C_1 symmetries; > 260 → 400 K: 2 independent molecules with C_2 symmetries; > 400 K: 1 independent molecule with C_2 (or D_2) symmetry. The gain in point symmetry is paralleled by a gain in mobility of the ligand (for example rotations of *tert*-butyl groups around the O−C axes), but so far we have not found a clear hint from the temperature-dependent ^{13}C-MAS NMR spectra that the sodium atoms are moving like the Li in the $\mathbf{Li_2Z_2}$ compound.

The compounds $Li_2[Ph{-}O{-}SiMe_2NSiMe_2{-}O{-}Ph]_2$ [$\mathbf{Li_2Z_2'}$] and $Li_2[Me_3Si{-}O{-}SiMe_2NSiMe_2{-}O{-}SiMe_3]_2$ [$\mathbf{Li_2Z_2''}$] differ from $\mathbf{Li_2Z_2}$ in that the *tert*-butyl group of $\mathbf{Li_2Z_2}$ is replaced by phenyl and trimethylsilyl groups, respectively. $\mathbf{Li_2Z_2'}$ forms a normal van der Waals lattice at ambient temperature ($P{-}1$ with Z = 2), and there are no other low- or high-temperature phases within ±120°C.[16] The molecules (isostructural with $\mathbf{Li_2Z_2}$) are dimeric with a central Li_2N_2 square, the Li−N distances being in the usual range of 2.061−2.097 Å.[25] The four Li−O distances are shorter than the Li−N distances, and have a mean value of 1.978(7) Å. In contrast with the phenyl derivative, the trimethylsilyl derivative $\mathbf{Li_2Z_2''}$ has long LiO distances [mean: 2.08(5) Å] and smaller Li−N distances [mean: 2.02(4) Å], but is similar to $\mathbf{Li_2Z_2}$ and $\mathbf{Li_2Z_2'}$ in its molecular structure. $\mathbf{Li_2Z_2''}$ crystalliszes in a monoclinic crystal system ($P2_1/c$ with Z = 4), and has a peculiar property when heated over 290 K. Its ^{13}C-MAS NMR spectrum becomes more simple, the multiple signals of the dimethylsilyl group of the room-temperature spectrum merging to two broad signals (δ = 5.0 and 7.1), and the four signals of the trimethylsilyl group changing into a singlet at δ = 2.7. This is a clear indication that ligand motions have to be considered, perhaps even accompanied by lithium hopping. At 355 K the spectrum becomes even simpler, with singlets for the dimethylsilyl and the trimethylsilyl groups. Unfortunately, until now, it has not been possible to obtain crystallographic proof for these assumptions.

We have also modified the O−Si−N−Si−O back bone by replacing O by other non-metallic elements such as nitrogen and carbon.[16] The following molecules have been prepared: $Li_2[Ph{-}SiMe_2NSiMe_2{-}Ph]_2$, $Li_2[(C_4H_3O){-}SiMe_2{-}N{-}SiMe_2{-}(OC_4H_3)]_2$, $Li_2[Me_2N{-}SiMe_2{-}N{-}SiMe_2{-}NMe_2]_2$, $Li_2[Et_2N{-}SiMe_2{-}N{-}SiMe_2{-}NEt_2]_2$, $Li_2[iPr(H)N{-}SiMe_2{-}N{-}SiMe_2{-}N(H)iPr]_2$, and $Li_2[(C_4H_3S){-}SiMe_2{-}N{-}SiMe_2{-}(SC_4H_3)]_2$. All these compounds show very similar structures to $\mathbf{Li_2Z_2}$, $\mathbf{Li_2Z_2'}$, or $\mathbf{Li_2Z_2''}$, but none of these compounds has been found to give several solid crystalline phases. In summary, the lithium hopping or rotational movement found thus far has been restricted to the O−Si−N−Si−O back bone.

Siloxamides with the Skeleton N−Si−O−Si−N

The Lithium and Sodium Derivatives of $[Me_3E{-}N{-}SiMe_2{-}O{-}SiMe_2{-}N{-}EMe_3]^{2-}$, E = C, Si

As shown in the last chapter, the motion of the lithium atoms within the compound $\mathbf{Li_2Z_2}$ in the crystalline solid had a direct link to the empty holes within the molecules. Occupying these holes by further metal atoms should prevent the jumping of the metal atoms, and therefore the metal rotation should stop.

With this idea in mind we have exchanged the places of the oxygen and nitrogen atoms in the skeleton O−Si−N−Si−O. To maintain the number of electrons, the skeleton N−Si−O−Si−N has to adopt a further negative charge, raising the total charge to −2. Two of these ligands should therefore accommodate 4 positively charged metal atoms and consequently, assuming a similar general structure, should completely fill up the O_2N_2 coordination polyhedra.[17]

We have obtained crystalline solids of the compounds $Li_4[tBu{-}N{-}SiMe_2{-}O{-}SiMe_2{-}NtBu]_2$; $\mathbf{Li_4X_2}$, $Li_4[Me_3Si{-}N{-}SiMe_2{-}O{-}SiMe_2{-}N{-}SiMe_3]_2$; $\mathbf{Li_4L_2}$, $Na_4[tBu{-}N{-}SiMe_2{-}O{-}SiMe_2{-}NtBu]_2$; $\mathbf{Na_4X_2}$, and $Na_4[Me_3Si{-}N{-}SiMe_2{-}O{-}SiMe_2{-}N{-}SiMe_3]_2$; $\mathbf{Na_4L_2}$.[17] Between 190 and 380 K the compound $\mathbf{Li_4X_2}$ forms three crystalline phases, $\mathbf{Na_4X_2}$ two crystalline phases, and both $\mathbf{Li_4L_2}$ and $\mathbf{Na_4L_2}$ one unique crystalline phase. Except the low-temperature phase of $\mathbf{Li_4X_2}$ (powder diffraction) all phases have been analysed by single-crystal X-ray diffraction (see Table 3). Solid-state NMR spectra have been obtained for all compounds using ^{6}Li, ^{7}Li, ^{13}C, ^{29}Si in the temperature-dependent mode.

In Figure 6 and Figure 7 the results of the X-ray diffraction analyses on $\mathbf{Li_4L_2}$ and $\mathbf{Na_4L_2}$ at room temperature are depicted.[17] As may be deduced by comparison of $\mathbf{Li_4L_2}$ with $\mathbf{Li_2Z_2}$ (Figure 1 and 2) the overall structures are quite similar, with the metallic cations connecting the negatively charged ligands. As anticipated the four O_2N_2 coordination holes which originate like in $\mathbf{Li_2Z_2}$ from the mutual orientation of the ligands are filled. Surprisingly, the lithium atoms are not found at distinct places but occupy two sites in the polyhedra with 50% probability and which are 0.66 Å apart from one another. The crystal symmetry of the molecules in $\mathbf{Li_4L_2}$ is S_4, which means that all four coordination sites as well as the lithium atoms are symmetry-related.

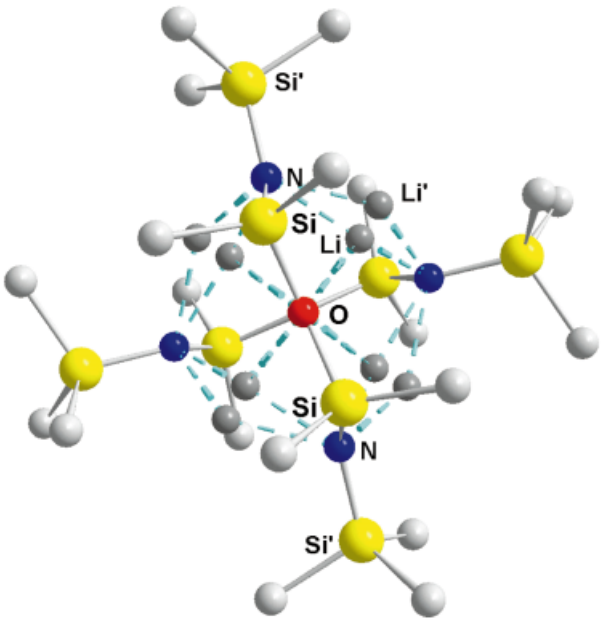

Figure 6. The molecular structure of $[Me_3Si-N-SiMe_2-O-SiMe_2-N-SiMe_3]_2Li_4$ (**Li_4L_2**) in the crystal at 290 K; the occupancy of the eight lithium positions is 50% (split atoms)

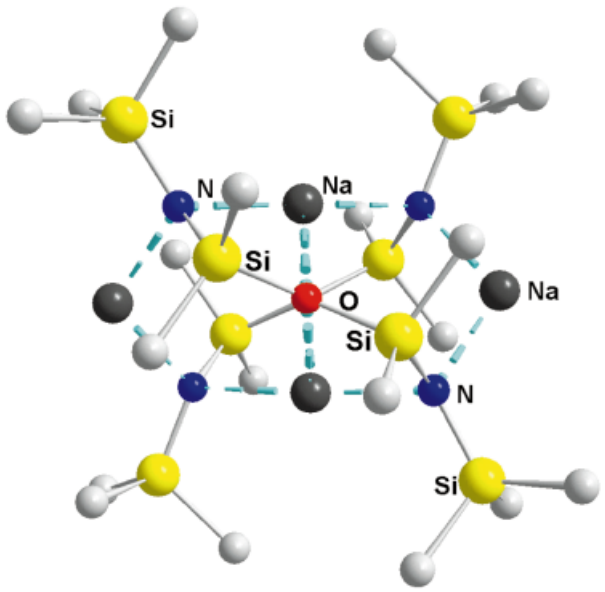

Figure 7. The molecular structure of $[Me_3Si-N-SiMe_2-O-SiMe_2-N-SiMe_3]_2Na_4$ (**Na_4L_2**) in the crystal at 290 K

What is the reason for equal distribution of four lithium atoms over eight sites in **Li_4L_2**? A closer look on the LiLi distances reveals that the inner sites, having the closest Li−O and Li−N distances [2.28(1) and 1.95(2) Å, respectively], are 2.37 Å apart. This distance should lead to a strong Li^+Li^+ repulsion, as may be deduced by a simple molecular mechanics calculation in the gas phase, or by comparison with other Li compounds (for the model calculation the lithium atoms have been assumed to have a charge of +1.0, and the N and O atoms −0.75 and −0.50, respectively).[20] Considering a combination of two inner and two outer sites of the lithium positions, the LiLi distances are increased to 2.91 Å and the Li^+Li^+ repulsions are consequently decreased. The outer sites of the lithium atoms show longer Li−N (2.037 Å) and Li−O distances (2.77 Å). Apparently there is a balance between the repulsion of the lithium atoms and the attraction from the O_2N_2 polyhedra. It seems likely that the splitting of the lithium positions is due to dynamical disorder with the two lithium sites representing the "return points" of lithium oscillations. This assumption can be verified as shown in the later sections.

The sodium derivative **Na_4L_2** is, to a crude approximation, similar to **Li_4L_2** and **Na_2Z_2**, as far as the general structure of the molecule is concerned. Closer inspection of Figure 7 nevertheless reveals that there are important differences. In contrast to the $S_4(\bar{4})$ symmetry of **Li_4L_2** the molecule **Na_4L_2** has no crystal symmetry but approaches $D_2(222)$ very closely. As a direct consequence of this different point symmetry, the four sodium atoms fall into two categories with two sodium atoms being coordinated by four basic atoms (two nitrogen and two oxygen atoms), and the other sodium atoms being coordinated only by two nitrogen atoms (not considering hydrogen interactions of CH_3 groups of the dimethylsilyl and trimethylsilyl entities). The dicoordinated sodium atoms have smaller Na−N distances when compared to the tetracoordinate (see Table 3) as expected. The N−SiSi−N dihedral angle in **Na_4L_2** is considerably larger than the corresponding angle in **Li_4L_2** (Table 3), and parallels our findings in the systems **Na_2Z_2** and **Li_2Z_2**. Another similarity to the former chapter is that in **Na_4L_2** there is no sodium movement, while in **Li_4L_2** lithium oscillations have to be considered.

Replacing the silicon atoms of the trimethylsilyl groups by the more electronegative carbon atoms should reduce the electron density at the nitrogen atoms. It should also reduce the ligating property of the nitrogen atoms to electropositive elements like Li or Na, and consequently should give more motional freedom to these atoms.

In Figure 8 the molecular structures of **Li_4X_2** and **Na_4X_2** are given either below 230 K or at ambient temperature as results of single-crystal X-ray diffraction analyses. It becomes evident, by comparison with Figure 6 and 7, that at lower temperatures, the structures of **Li_4X_2** and **Na_4X_2** compare almost perfectly with the structures of **Li_4L_2** and **Na_4L_2** (see also Table 3). The contrary is true for the structures determined at ambient temperature: Here the structural features are different, the crystal point symmetry of **Li_4X_2** being $D_{2d}(\bar{4}2m)$, and of **Na_4X_2** being $S_4(\bar{4})$. In the two cases the *tert*-butyl groups of the ligands are disordered around the C−O axes as result of rotational dynamics (which can be verified by solid-state ^{13}C NMR).

The LiLi separation of the two split positions is becoming longer by 0.13 Å in the room temperature phase [**Li_4X_2** (230 K): LiLi = 0.81 Å; **Li_4X_2** (290 K): LiLi = 0.94 Å] compared with that at 230 K. This is in accord with the model of Li oscillations becoming more important with raising temperature. A careful look at the electron-density map of the crystal-structure determination of **Li_4X_2** (290 K) reveals that other atoms of the compound besides lithium are

Table 3. Some selected bond lengths [Å], angles [°] and symmetry information for compounds with the backbone N−Si−O−Si−N

	Si−N	Si−O	N−Si···Si−N[a]	M−N[b] {N−M−N}	M−O	MM[c]	Symmetry[d] Space group [Z]
Li_4X_2 (296K)	1.669(4)	1.662(2)	0.0	1.917(3) 2.019(6)	2.37(1)	2.75(2) 2.03(2) min	***D_{2d}*** [D_{2d}] $P4_2/nmc$ [2]
Li_4X_2 (230K)	1.667(4)	1.655(2)	13.7(1)	1.93(1) 1.91(1)	2.49(2)	2.71(3) 2.09(2) min	***S_4*** [S_4] $P4_2/n$ [2]
Li_4L_2	1.685(2)	1.659(1)	27.5(1)	1.93(1) 1.97(1) 2.05(1) 2.03(1)	2.28(1)	2.91(2) 2.37(2) min	***S_4*** [S_4] $P4_2/n$ [2]
Na_4X_2 (296K)	1.655(5)	1.670(2)	44.9(1)	2.322(5) 2.311(5)	2.613(4)	3.240(5)	***S_4*** [S_4] $P4_2/n$ [2]
Na_4X_2 (200K)	1.652(6)	1.659(9)	36.6(1)	2.34(1) {178.1°} 2.36(1) {121.2°}	2.571(9)	3.172(5) 3.485(3)[×4]	**D_2** [C_1] $Pna2_1$ [4]
Na_4L_2	1.670(6)	1.675(8)	48.5(1)	2.416(9) {177.1°} 2.368(9) {116.1°}	2.507(9)	3.249(3) 3.689(3)[×4]	***D_2*** [C_1] $P2_1/n$ [4]
$Li_2K_2X_2$	1.659(5)	1.673(5)	10.5(1)	2.769[K] 1.959[Li]	2.395[Li]	2.95[Li−Li] 3.56[Li−K]	***D_2*** [C_2] $Aba2$ [4]
Cu_4X_2	1.721(5)	1.642(4)	11.2(1)	2.156(3) {165.0°}	3.08 [no bonding]	2.836(3)	***D_{2d}*** [C_2] $C2/c$ [4]
Ag_4X_2	1.729(5)	1.630(4)	11.7(1)	2.153(3) {165.2°}	3.11 [no bonding]	2.834(2)	***D_{2d}*** [C_2] $C2/c$ [4]

[a] Dihedral angle Si−N···N−Si in °. – [b] M−N distances and, in some compounds, corresponding N−M−N angles. – [c] Shortest distances between metal centres using inner and outer split atom positions; the values characterized by "min" show the shortest unrealistic distances. – [d] In the first line are point symmetries (bold: approximate; in brackets: crystal site symmetry). The second line gives the space groups with the number of molecules per unit cell in brackets.

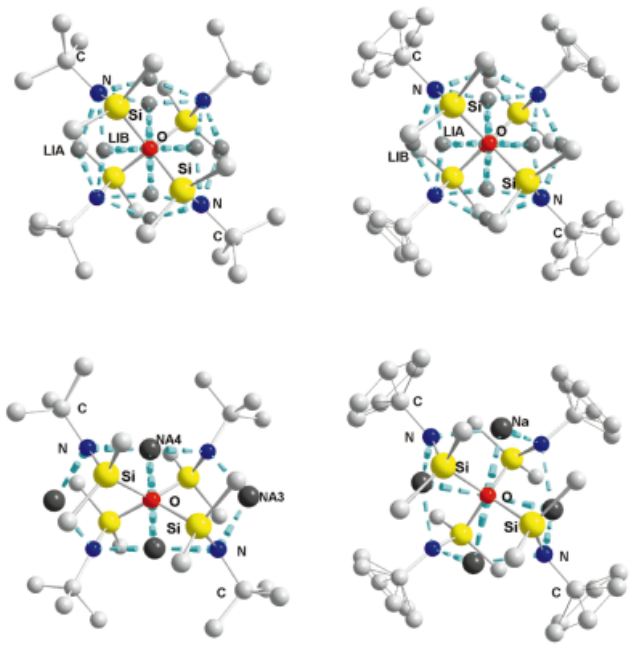

Figure 8. Comparison of the structures of [*t*Bu−N−SiMe$_2$−O−SiMe$_2$−N−*t*Bu]$_2$M$_4$, M = Li, Na (**Li_4X_2**, **Na_4X_2**) at different temperatures; on the left the low-temperature phases (200 K) are plotted, while on the right the same molecules are shown at ambient temperature

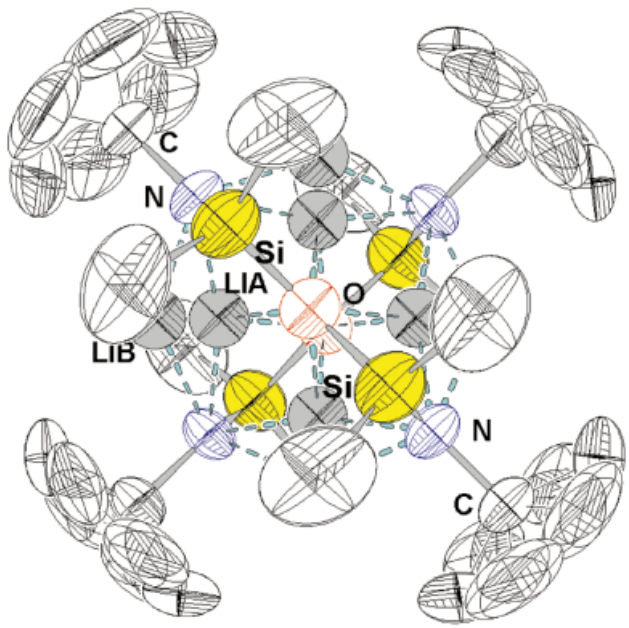

Figure 9. Molecular structure of Li$_4$[*t*Bu−N−SiMe$_2$−O−SiMe$_2$−N*t*Bu]$_2$ (**Li_4X_2**) at 290 K showing ellipsoids of thermal motion (50%)

"smeared out" (as may be seen from Figure 9 showing the anisotropic ellipsoids).

From Figure 9 it can also be concluded that apart from the rotations of the *tert*-butyl groups, the most important movement is that of the dimethylsilyl group that is perpen-

dicular to the mirror planes of the D_{2d} point symmetry. The phase transition of $\mathbf{Li_4X_2}$ (230 K) to $\mathbf{Li_4X_2}$ (290 K) has a direct group/subgroup relation ($P4_2/n \xrightarrow{t2} P4_2/nmc$): This is a serious hint for the presence of a second-order transition, which can be followed by spectroscopic techniques like NMR and Raman spectroscopy (see later).

The temperature-dependent structure change of $\mathbf{Li_4X_2}$ may be described as follows: At 230 K the molecules are highly librating in the crystal lattice, the movements becoming more important at higher temperatures. The most important amplitudes of movement are the lithium oscillations, followed by rotations of the *tert*-butyl groups and dimethylsilyl displacements perpendicular to the ON_2 plane of the ligand $[t\mathrm{Bu-N-SiMe_2-O-SiMe_2-N-}t\mathrm{Bu}]^{2-}$. A measurable quantity for the dimethylsilyl motion is the N−SiSi−N dihedral angle, which at 230 K has an equilibrium value of 13.7°. With raising temperature the dihedral value approaches 0°, corresponding with the equilibrium value of the high-temperature phase. The high molecular point symmetry D_{2d} is finally reached above 260 K (see NMR experiments) with free rotation of the *tert*-butyl groups. In the phase transition the N−SiSi−N angle can be defined, inter alia, as an ordering parameter.

The point symmetry of $\mathbf{Li_4X_2}$ (230 K) is $S_4(\bar{4})$, and from a packing point of view is not ideal for organic molecules.[21] It is not astonishing that at lower temperatures another crystalline phase for $\mathbf{Li_4X_2}$ is found which is stable below 170 K [$\mathbf{Li_4X_2}$ (160 K)]. We were not able to obtain single crystals from this phase, but have deduced from X-ray powder diffraction that the crystal system is lower than tetragonal, and could be orthorhombic or monoclinic.

The $\mathbf{Na_4X_2}$ compound shows two crystalline phases, the molecular structures of the compounds being quite different as may be concluded from Figure 8. At ambient temperature $\mathbf{Na_4X_2}$ crystallizes in the tetragonal lattice in space group $P4_2/n$ with $Z = 2$ as $\mathbf{Li_4X_2}$ at 230 K, and below 240 K $\mathbf{Na_4X_2}$ becomes orthorhombic (space group $Pna2_1$). While in the low-temperature phase the molecule has crystal point symmetry C_1 but deviates only a little from $D_2(222)$, in the high-temperature phase of $\mathbf{Na_4X_2}$ the crystal point symmetry is $S_4(\bar{4})$ (Table 3). In the low-temperature phase of $\mathbf{Na_4X_2}$ there are two types of sodium atoms, as in $\mathbf{Na_4L_2}$, and the structures of these two phases are very similar, omitting the *tert*-butyl/trimethylsilyl exchange. With respect to O and N in $\mathbf{Na_4X_2}$ (220 K) there are λ^2- and λ^4-Na atoms, while in $\mathbf{Na_4X_2}$ (290 K) all Na atoms are three-coordinate (see also Table 3). The phase transition in the Na_4X_2 system is of first order (vide NMR): The change in the molecular structure thus happens instantaneously.

The structural change in $\mathbf{Na_4X_2}$ associated with the phase transition from low to high temperature has three characteristics: (1) The sodium atoms become equivalent and change from $2 \times \lambda^2$-Na and $2 \times \lambda^4$-Na to $4 \times \lambda^3$-Na. The vibrations of the sodium atoms become stronger, but there is no evidence for a sodium oscillation as in the case of $\mathbf{Li_4X_2}$. (2) The different point symmetry of the molecule at higher temperature is accompanied by a substantial gain in volume [increase in volume/molecule = 34.6 Å^3 (3.6%); in the $\mathbf{Li_4X_2}$ system (230/290 K) the volume increase is 20.0 Å^3 (2.2%)]. This increase is used for rotational freedom of the *tert*-butyl groups. (3) The mutual orientation of the $[t\mathrm{Bu-N-SiMe_2-O-SiMe_2-N-}t\mathrm{Bu}]^{2-}$ ligands is changed, and the dihedral angles N−SiSi−N increase from 36.6° for $\mathbf{Na_4X_2}$ (220 K) to 44.9° for $\mathbf{Na_4X_2}$ (290 K). Whereas at 220 K the two ligands are symmetry-related by C_2 and have the same twisting direction (along the N−Si−O−Si−N skeleton), at 290 K the ligands have opposite twists. This is best seen by closer inspection of Figure 8.

In conclusion, the two phase transitions studied with $\mathbf{Li_4X_2}$ and $\mathbf{Na_4X_2}$ with X-ray diffraction techniques are similar with respect to obtaining motional freedom for the *tert*-butyl groups with increase in the temperature, but the effect on the metal atoms is different. While in the case of lithium the oscillations along two of the twofold axes of the D_{2d} symmetry become more important with increase in temperature, in the case of sodium there is one important displacement of these atoms at the transition point, without any further metal movements. The silicon derivatives $\mathbf{Li_4L_2}$ and $\mathbf{Na_4L_2}$ at ambient temperatures have molecular structures that can only be realised in $\mathbf{Li_4X_2}$ and $\mathbf{Na_4X_2}$ at lower temperatures. This is a direct consequence of the different charge distributions at nitrogen due to carbon/silicon exchange. The nitrogen atoms in $\mathbf{Li_4L_2}$ and $\mathbf{Na_4L_2}$ are more negatively charged than the same atoms in the $\mathbf{Li_4X_2}$ and $\mathbf{Na_4X_2}$ derivatives and therefore hinder the motional freedom of the metal atoms by a higher electrostatic component.

The models discussed so far have been checked by solid-state NMR. In Figure 10 and Figure 11 the ^{13}C-NMR spectra of $\mathbf{Li_4X_2}$ and $\mathbf{Na_4X_2}$ in the temperature range between 150 and 350 K are shown. In exact correspondence to the X-ray diffraction results the phase transitions in both systems are easily recognised, and temperatures of transition are paralleled. In the $\mathbf{Li_4X_2}$ system, starting with 150 K, the first transition occurs at 165 K. Below 165 K the ^{13}C-MAS NMR spectrum is highly structured especially in the dimethylsilyl region. Here at least six different signals can be recognised, which collapse at 165 K to two signals of equal intensity. From the number of signals it can be deduced that the point symmetry of the $\mathbf{Li_4X_2}$ below 165 K is less than C_2 and is most probably C_1 (8 signals are expected for this point symmetry). The broad peak of the primary carbon atoms in the *tert*-butyl groups hints at an ordered structure, ruling out any rotational movement. The spectral change at 165 K is sudden, in accord with a first order transition.

Above 168 K the spectrum of $\mathbf{Li_4X_2}$ is constantly changing with two major observations: (1) The intensity of the *tert*-butyl signal (methyl groups) with respect to the dimethylsilyl group is gradually increasing: This effect can be attributed to an initial rotation of the *tert*-butyl groups around the C−N axis becoming more and more important. (2) The space separation of the two methyl groups is almost constant between 165 K and 205 K. Between 205 K and 245 K the separation is constantly diminishing, the intensity of the signal growing and finally collapsing to a singlet at

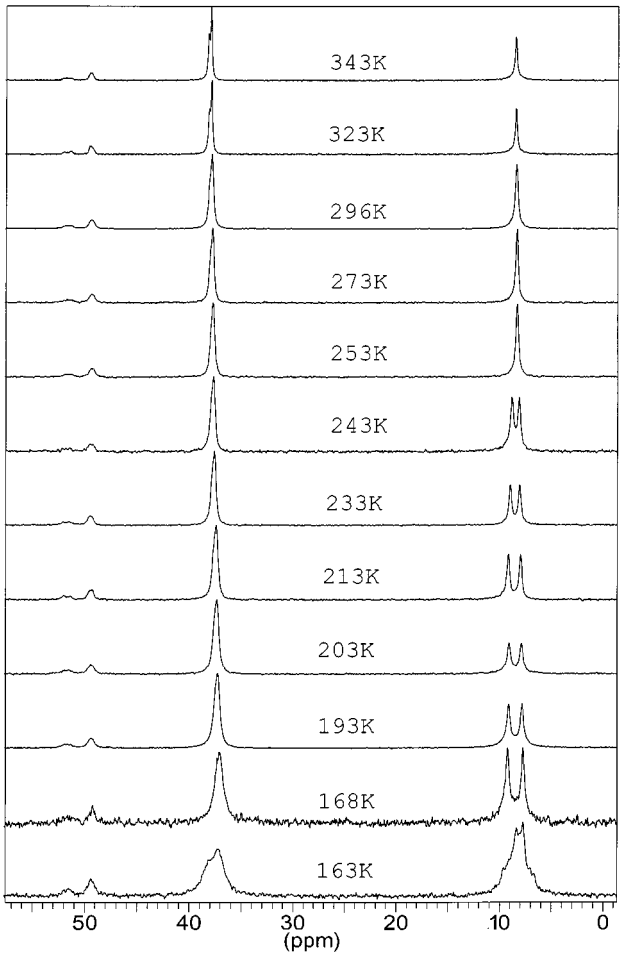

Figure 10. ^{13}C-MAS NMR spectrum of $\mathbf{Li_4X_2}$ between 150 and 350 K

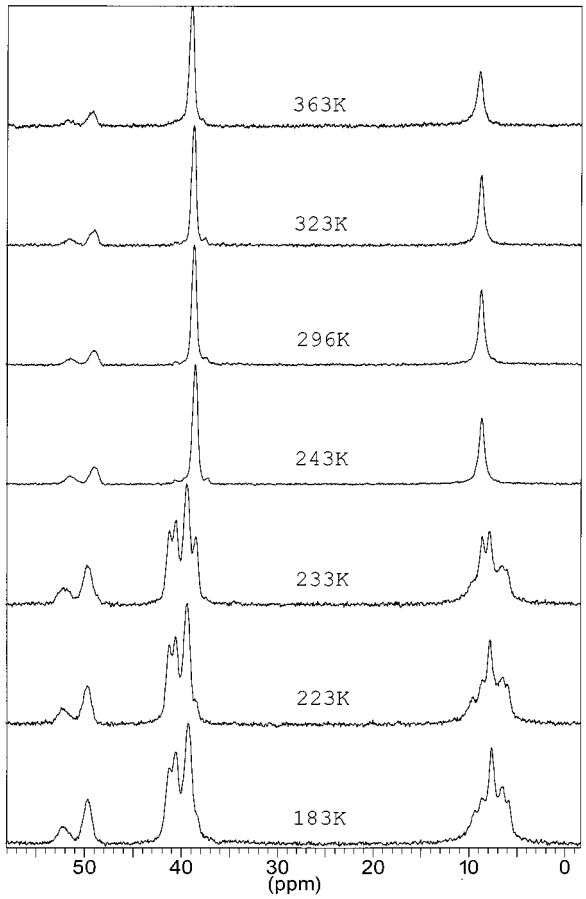

Figure 11. ^{13}C-MAS NMR spectrum of $\mathbf{Na_4X_2}$ between 150 and 350 K

245 K. The experiment seems to reflect the starting libration of the dimethylsilyl groups in the crystal, which become more and more intense with the N−SiSi−N dihedral angle approaching 0° (see before). It also confirms our assumption that the phase transition between $\mathbf{Li_4X_2}$ (230 K) and $\mathbf{Li_4X_2}$ (290 K) is of second order with a continuous change of parameters. It is interesting to note that the crystallographic S_4 symmetry is nicely reflected in the spectrum with one independent *tert*-butyl group and two independent methyl groups in the Me_2Si region.

Above 245 K the spectrum of $\mathbf{Li_4X_2}$ is in accordance with the crystallographic $D_{2d}(\bar{4}2m)$ symmetry, and two signals for all methyl groups within the molecule are measured. The tertiary carbon atom of the *tert*-butyl group is not affected during the phase transitions, as can be seen from Figure 10. This is due to the central position of the carbon atom which is shielded and suffers to a smaller extent from structural changes than a carbon atom situated on the outer sphere of the molecule. The two asymmetric resonances of the primary carbon atom are due to the quadrupole splitting of the nitrogen to which it is attached.

We have been lucky, to follow the phase transitions in $\mathbf{Li_4X_2}$ also by single-crystal Raman spectroscopy.[22] In Figure 12 a section of the spectrum (2600−3000 cm^{-1}) is shown, which has been obtained from a crystal oriented orthogonal to the [001] direction of the tetragonal phase.

The highest frequency of the C−H stretching modes is especially sensitive to the phase transition: At 150 K the signal at 2950 cm^{-1} is definitely different from the corresponding one at 160 K, which with increasing temperature is gradually changing. Very recently we have obtained a DSC curve of the phase transition around 245 K, which is shown in Figure 13.[26]

The λ curvature of the plot is reminiscent of the ideal second-order phase transition, the original model description being developed by P. Ehrenfest and L. D. Landau.[27] In conclusion, the Raman spectroscopy as well as the DSC experiment fully parallel our NMR and X-ray experiments and substantiate our earlier assumptions.

The solid-state ^{13}C-NMR experiments with $\mathbf{Na_4X_2}$ are not as straightforward as with $\mathbf{Li_4X_2}$ (Figure 11).

In accordance with the low crystal symmetry of the $\mathbf{Na_4X_2}$ molecule, in between 180 K and 220 K the Me_2Si group (at least 5 signals) and the *tert*-butyl groups (at least 3 signals) show up as multiplets. At 233 K the multiplets become more complex by addition of a further line to each of them. As can be deduced from the spectrum at 243 K, the additional peaks are from the high-temperature tetragonal phase. There is a coexistence of the two phases (orthorhombic and tetragonal) in accord with the first-order

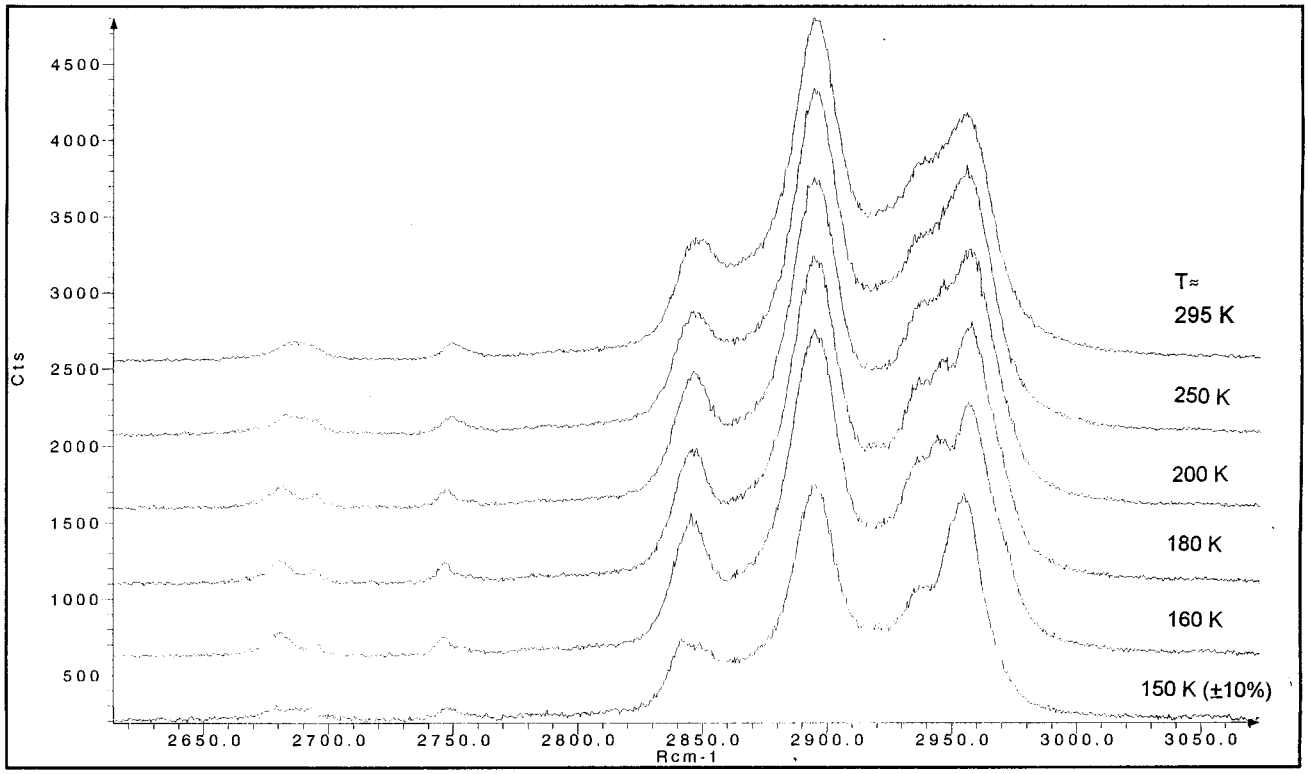

Figure 12. Section of Raman spectrum of $\mathbf{Li_4X_2}$ (2600−3100 cm^{-1}) at different temperatures (single crystal)

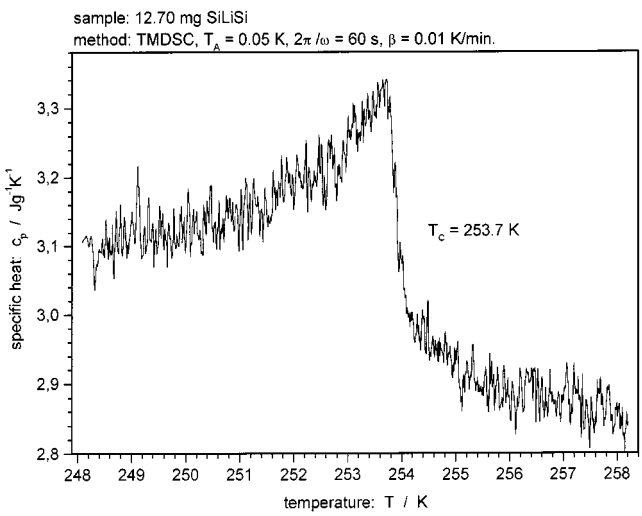

Figure 13. The "λ-transition" at 245 K found by micro-DSC for $\mathbf{Li_4X_2}$

phase transition. Above 233 K the spectrum of $\mathbf{Na_4X_2}$ is very simple, with two resonances for the *tert*-butyl and dimethylsilyl group and the quadrupolarly coupled tertiary carbon atom.

There is clearly a misfit between the X-ray results and the ^{13}C-NMR spectrum for the high-temperature phase of $\mathbf{Na_4X_2}$. As in the corresponding $\mathbf{Li_4X_2}$ (230 K) spectrum, the dimethylsilyl group should show up as two signals of equal intensity [in accordance with the $S_4(\bar{4})$ point symmetry]. What could be the reason for the observed singlet? There are several possibilities. As the signal of the high-temperature phase of $\mathbf{Na_4X_2}$ is very broad (the signal half-width broadness is double that of the corresponding $\mathbf{Li_4X_2}$ phase), the experiment could suffer from lack of resolution. Unfortunately, changing the experimental parameters (using a 500-MHz NMR equipment instead of a 200-MHz one) does not reveal any new insight, as the signal remains comparatively broad but is not structured. Another possible explanation could be that the X-ray structure solution of the tetragonal phase is wrong, due to undiscovered twinning. We are still in the process of proving or disproving these assumptions.

Besides ^{13}C-NMR techniques, ^{6}Li-, ^{7}Li-, and ^{29}Si NMR have also been used to follow the phase transitions (in $\mathbf{Li_4X_2}$ and $\mathbf{Na_4X_2}$). The most interesting is of course the Li NMR, as we could obtain direct information on the lithium mobility. To cut a long story short, two main observations have been made: (1) From the broad-line powder spectra the asymmetry parameter of the lithium position in $\mathbf{Li_4X_2}$ can be obtained. It changes from 0.11 at 150 K to 0.05 at 230 K and remains constant until 360 K, which is an accord with obtaining more axial symmetry (C_2). (2) Within the temperature range of 230 to 260 K the spinning side bands of the MAS spectra show a notable line broadening and consequently a reduced MAS sensitivity.[28] This dynamically induced line broadening seems to be a direct trace of the lithium movement. Above 270 K the spinning side bands sharpen again due to the increasing frequency of the molecular motion (see Figure 14).

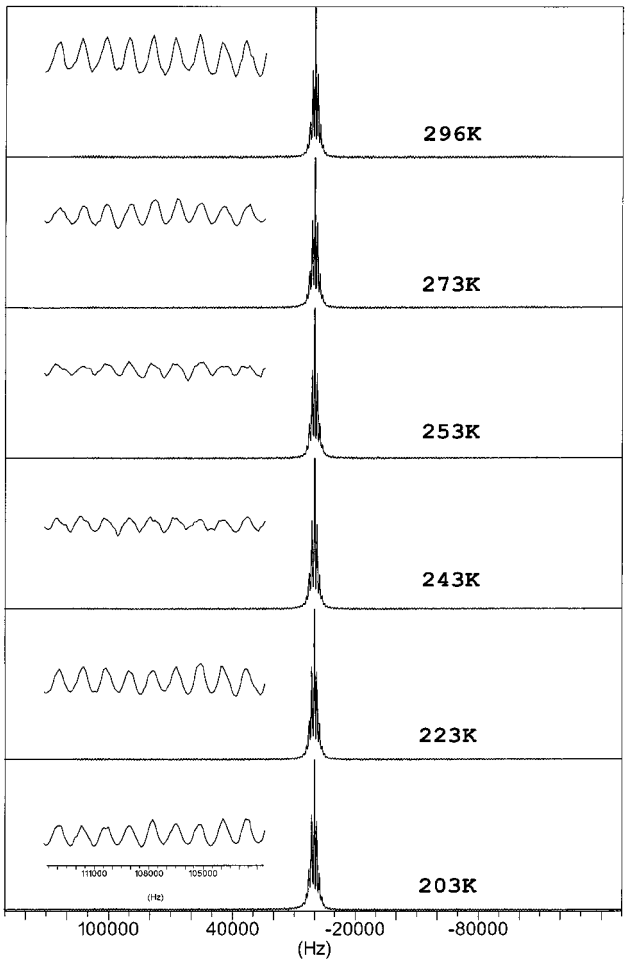

Figure 14. ^{7}Li-MAS spectra of $\mathbf{Li_4X_2}$; the expanded region of the spinning side bands shows the homogeneous line broadening with reduced efficiency of the MAS experiment at the phase transition

The N−Si−O−Si−N Skeleton with Different Substituents

Whereas in the last chapter the mobility of the lithium and sodium atoms has been shown to be influenced by a C/Si exchange at the nitrogen atoms of the N−Si−O−Si−N skeleton, in this chapter we present our results from more dramatically changing the substituents on the whole skeleton. Although we have followed these experiments by spectroscopic means, we only present the X-ray results.

The ligand [*t*Bu−SiMe$_2$−N−SiMe$_2$−O−SiMe$_2$−N−SiMe$_2$−*t*Bu]$^{2-}$ can be derived from [Me$_3$Si−N−SiMe$_2$−O−SiMe$_2$−N−SiMe$_3$]$^{2-}$ by exchange of a methyl group by the sterically demanding *tert*-butyl group at the outer silicon atoms. The compound [*t*Bu−SiMe$_2$−N−SiMe$_2$−O−SiMe$_2$−N−SiMe$_2$−*t*Bu]$_2$Li$_4$, $\mathbf{Li_4L'_2}$, has been analysed by X-ray diffraction, the result being shown in Figure 15.[17] Interestingly, even at room temperature, the lithium atoms are at rest and the structure obtained is quite different from $\mathbf{Li_4L_2}$. The molecule $\mathbf{Li_4L'_2}$ adopts almost D_2(222) symmetry in the crystal (exact crystal symmetry C_1) with two pairs of different lithium atoms (λ^2-Li and λ^4-Li). The λ^2-Li atoms have further contacts with the methyl groups of the *tert*-butyl and the dimethylsilyl groups (LiC 3.0 Å), which explains nicely the stability of the structure.

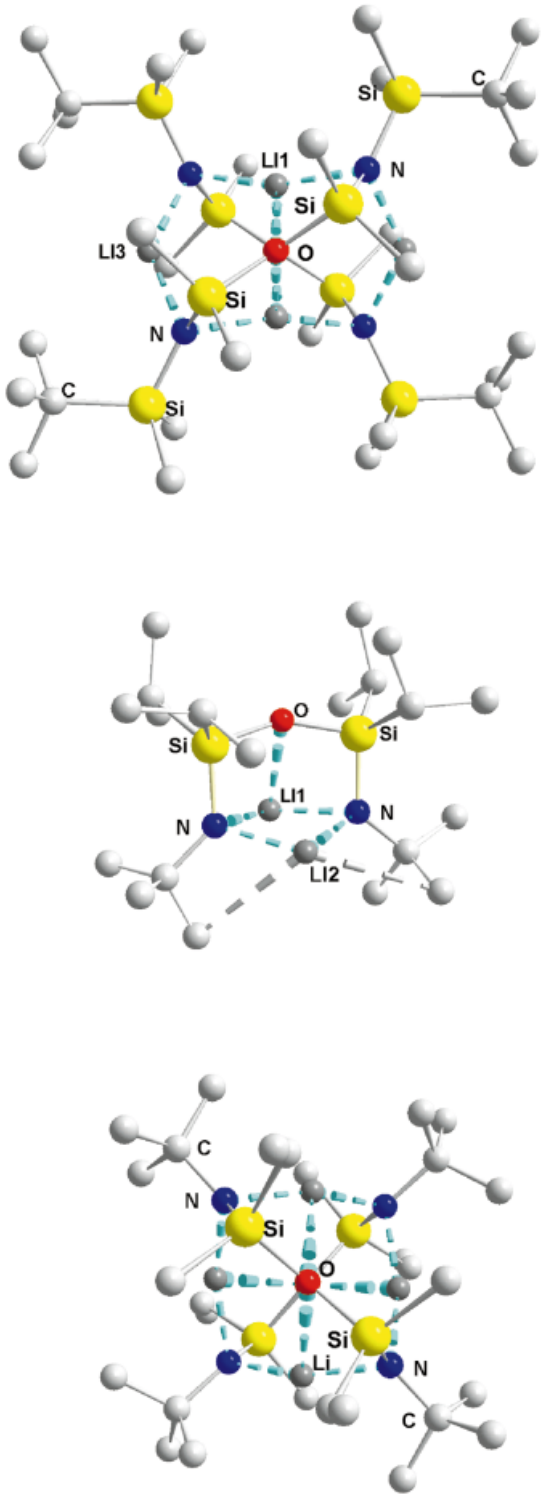

Figure 15. Molecular structures at 290 K of Li$_4$[*t*Bu−SiMe$_2$−N−SiMe$_2$−O−SiMe$_2$−N−SiMe$_2$−*t*Bu]$_2$ ($\mathbf{Li_4L_2}$), Li$_2$[*t*Bu−N−Si(*i*Pr)$_2$−O−Si(*i*Pr)$_2$−N*t*Bu] ($\mathbf{Li_2X''}$), and Li$_4$[*t*Bu−N−Si(Me)(CH=CH$_2$)−O−Si(Me)(CH=CH$_2$)−N−*t*Bu]$_2$ ($\mathbf{Li_4X_2}$)

It seems likely that steric as well as electronic effects are responsible for the difference in the structure of $\mathbf{Li_4L_2'}$ compared with that of $\mathbf{Li_4L_2}$.

The steric influence can also be observed when the methyl groups at the silicon atoms of [*t*Bu−N−

$SiMe_2-O-SiMe_2-N-tBu]^{2-}$ are replaced by bulkier groups like isopropyl moieties. The corresponding lithium derivative of this ligand $[tBu-N-Si(iPr)_2-O-Si(iPr)_2-N-tBu]Li_2$, **$Li_2X''$**, is no longer dimeric, but monomeric. The isopropyl groups on the silicon atoms seem to prevent dimerisation, and **Li_2X''** can be obtained in its monomeric form even in the crystal (Figure 15). The two lithium atoms are very different in their coordination, the λ^3-Li possessing a small Li−O contact (2.34A) and longer Li−N bonds [1.99(1) Å], while the λ^2-Li has shorter Li−N bonds [1.978(2)Å]. Besides these bonds the λ^2-Li has two narrow distances to carbon (2.99 Å).

When the organic substituents on the silicon atoms in $[tBu-N-SiR_2-O-SiR_2-N-tBu]^{2-}$ are different, the silicon atoms become chiral, and the whole ligand can either belong to the *R*,*R* (*S*,*S*) or *R*,*S* (*S*,*R*) enantiomer (*R* and *S* designing the chirality of the two silicon centres). In the first case, assuming a planar ligand, the point symmetry of the anionic ligand is $C_2(2)$ while in the second case it is $C_s(m)$. We have prepared several examples of these ligands (see Table 1), and to our great surprise have found, that the ligands with the *R*,*R* (*S*,*S*) chirality exclusively crystallize as lithium salts, while in the mother liquor both enantiomers are present (^{1}H-NMR evidence). In Figure 15 the structure of $[tBu-N-Si\{(Me)(CH=CH_2)\}-O-Si\{(Me)(CH=CH_2)\}-NtBu]_2Li_4$, **$Li_4X_2'$**, is shown. The molecule crystallizes in the tetragonal space group $P\bar{4}2_1c$ with two molecules per unit cell, and has the crystal point symmetry S_4. As a consequence, each lithium atom is in the same atom environment, and is coordinated by two nitrogen, two oxygen, and two carbon atoms. Each molecule contains one ligand with (*R*,*R*) chirality at Si and a second one with (*S*,*S*) chirality. The lithium oscillation (not shown in the Figure) is less important than in the corresponding compound **Li_4X_2**, and the atoms can be refined without splitting positions (but with large anisotropic temperature factors). The N−SiSi−N dihedral angle is 12.4°, but as the substituents on silicon are different, there is no energetically equivalent position in the other twist form (dihedral angle −12.4°) and the system seems to avoid the passage to the other conformer. This explains the fact that **Li_4X_2** and **Li_4X_2'** are quite different at the same temperature (290 K), **Li_4X_2** showing large lithium oscillations while **Li_4X_2'** only has small amplitudes.

We can conclude from these substitution experiments that the structures of the molecules and the motion of the metal atoms can be easily manipulated. The results fit in nicely in our atomistic dynamic models.

The N−Si−O−Si−N Skeleton with Different Metallic Elements

So far we have compared the lithium and sodium derivatives of the same ligands. The compound $Li_2K_2[tBuN-SiMe_2-O-SiMe_2-NtBu]_2$, **$Li_2K_2X_2$**, belongs to the family **Li_4X_2** and **Na_4X_4** with the peculiarity of hosting two types of metallic atoms. Looking back to the structures we have known so far, it seemed unlikely that **$Li_2K_2X_2$** should adopt the S_4 symmetry of the tetragonal phase of **Na_4X_2** or the

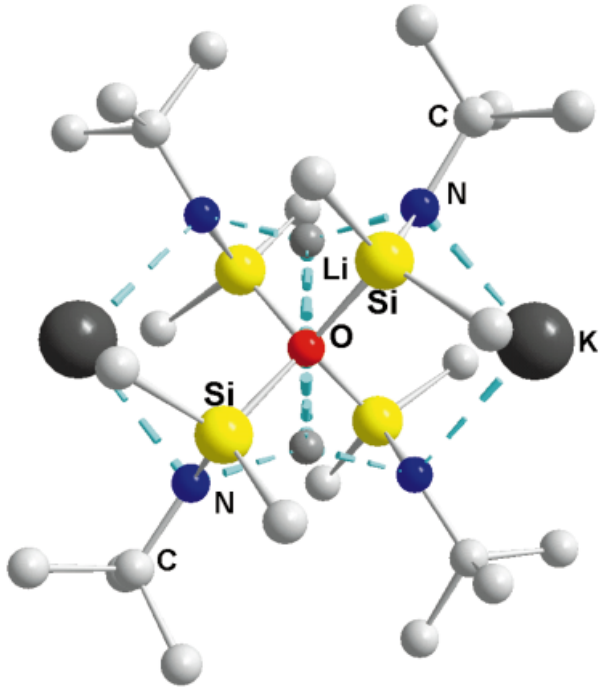

Figure 16. Molecular structure of $Li_2K_2[tBu-N-SiMe_2-O-SiMe_2-N-tBu]_2$ (**$Li_2K_2X_2$**) at 290 K in the solid; the smaller lithium atoms occupy the N_2O_2 holes while the bigger potassium atoms are situated on the outside

D_{2d} symmetry of the high-temperature phase of **Li_4X_2**. As a matter of fact, **$Li_2K_2X_2$** forms a structure very similar to the low-temperature phase of **Na_4X_2**, as can be seen from Figure 16.[17] Between 200 and 380 K we have found no hint for any phase transition as the ^{13}C-MAS NMR spectra remain unchanged.

While the smaller lithium atoms in **$Li_2K_2X_2$** occupy quasi-tetrahedral O_2N_2 holes, the two potassium atoms are too large to be accommodated in these coordination polyhedra and are only bonded by two nitrogen atoms. Furthermore, the potassium atoms have close contacts to carbon atoms of the *tert*-butyl ligands. The crystal symmetry of the whole molecule is C_2 (the two-fold axis passes through the lithium atoms), but the bond lengths and angles as well as the dispositions of the atoms reveal it to be close to D_2. As already discussed, **$Li_2K_2X_2$** is structurally similar to the orthorhombic phase of **Na_4X_2**. Contrary to this compound, no phase transition is observed as the two different elements are well accommodated in their respective coordination spheres. Comparing **$Li_2K_2X_2$** to **Li_4X_2** no lithium motion is observed in the former as there is no need to equilibrate between different lithium positions.

Other interesting cases to discuss are the monovalent transition metal derivatives $Cu_4[tBuN-SiMe_2-O-SiMe_2-NtBu]_2$, **$Cu_4X_2$**, and $Ag_4[tBuN-SiMe_2-O-SiMe_2-NtBu]_2$, **$Ag_4X_2$**. The two compounds have the same composition as **Li_4X_2** or **Na_4X_2** and are somewhat similar in their structures, but also show important differences to the alkali derivatives. In Figure 17, the structure of one of the two compounds, which are isotypic, is depicted as a result of an X-ray structure analysis.

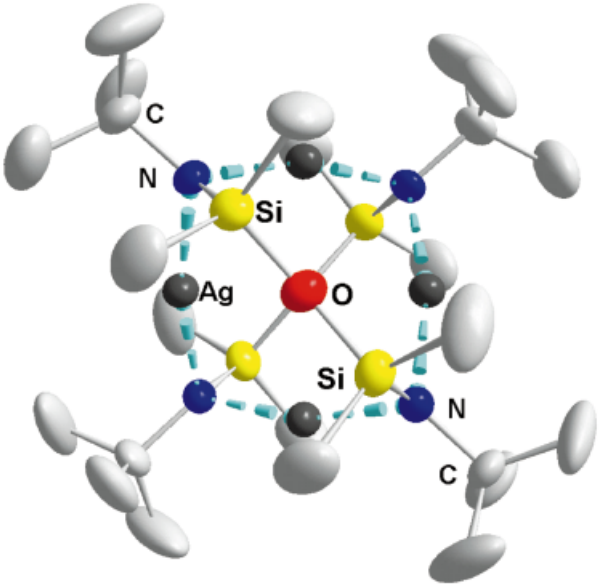

Figure 17. Molecular structure of $Ag_4[t\mathrm{Bu}-\mathrm{N}-\mathrm{SiMe}_2-\mathrm{O}-\mathrm{SiMe}_2-\mathrm{N}-t\mathrm{Bu}]_2$ (**Ag_4X_2**) with ellipsoids of vibration (50%) at 290 K

The crystal point symmetry of the compounds is $C_2(2)$ but the deviation from $D_{2d}(\bar{4}2m)$ is almost negligible (the N−SiSi−N dihedral angles are 11.2° in **Cu_4X_2** and 11.7° in **Ag_4X_2**). Although belonging to the same molecular point symmetry, compared to the ambient-temperature phase of **Li_4X_2**, **Cu_4X_2**, or **Ag_4X_2** are distinctly different in their structures. The N−M−N bonds are almost linear (**Cu_4X_2**: N−Cu−N = 164.9°; **Ag_4X_2**: N−Ag−N = 165.2°) and there are no bonding interactions of the metal centres with the oxygen atoms. Furthermore, the anisotropic displacement factors of the metal atoms in the compounds are small and there is no evidence for metal oscillations as in compound **Li_4X_2**. The different behaviour of the copper and silver atoms compared to lithium is due to a well-known reason: The metal atoms are in a preferred s(d)p-bond configuration and there are numerous examples of this bonding type in the literature.[29]

Conclusions

We have been able to show that metal movements, especially of lithium (cations), are possible within a molecular skeleton in a crystalline solid. The motions of these metal atoms (ions) are linked to phase transitions and rotations or oscillations of atoms or groups within the molecular skeleton. The phase transitions are reflecting the change of overall symmetry of the molecular movements. The large vibrations within the ligands are necessary to minimize the activation energy of the metal motion.

In the systems **M_2Z_2** it can be clearly shown that only the lithium atoms (or in an ionic model: ions) are capable to jump from filled holes into empty ones. This jumping leads to a rotational motion that may proceed backwards or

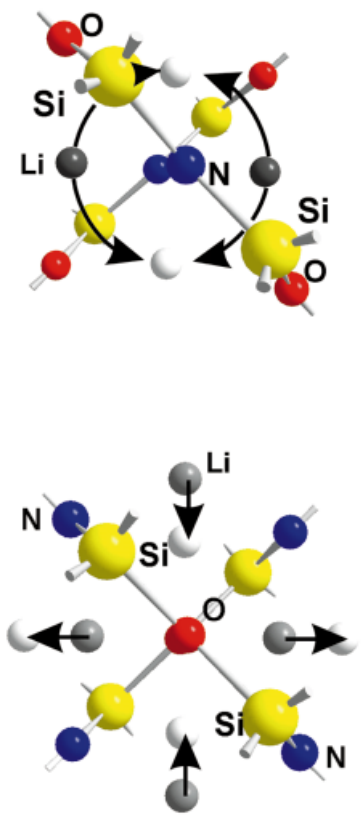

Figure 18. Comparison of the lithium movements within **Li_2Z_2** and **Li_4X_2** at ambient temperature. While in the case of **Li_2Z_2** there is a forward and backward rotation, in **Li_4X_2** there is a forward and backward oscillation; lithium positions are discriminated by white and grey colours; only one type of these coloured position is occupied at a time for electrostatic reasons

forwards (Figure 18). The rotational motion of the lithium atoms appears to be simultaneous, which means that the two metallic atoms within the molecule are jumping at the same time, because of electrostatic reasons. Although the sodium derivative also shows phase transitions to allow more motional freedom to the organic ligands, there is no evidence for a comparable sodium hopping or rotation. This leads to the conclusion that the lithium motion is perhaps better described as "lithium tunnelling". The trimethylsilyl derivative **Li_2Z_2**" has a structure very similar to **Li_2Z_2** in the monoclinic phase. Whereas the monoclinic phase of **Li_2Z_2** is stable up to 293 K, the monoclinic phase of **Li_2Z_2**" is stable up to 340 K. The higher charge transfer of the trimethylsilyl group to the oxygen atom compared to *tert*-butyl seems to be responsible for this effect.

The complete fill-up of the N_2O_2 holes in siloxamides by metallic atoms has been realised by the use of the skeleton N−Si−O−Si−N in the place of O−Si−N−Si−O. Although the rotational lithium hopping is stopped by this transformation, the system is still highly fluctional in the crystal, with lithium oscillations occurring along two of the three twofold axes of the $D_{2d}(\bar{4}2m)$ point symmetry (Figure 18). As in the case of **Li_2Z_2**, temperature-dependent

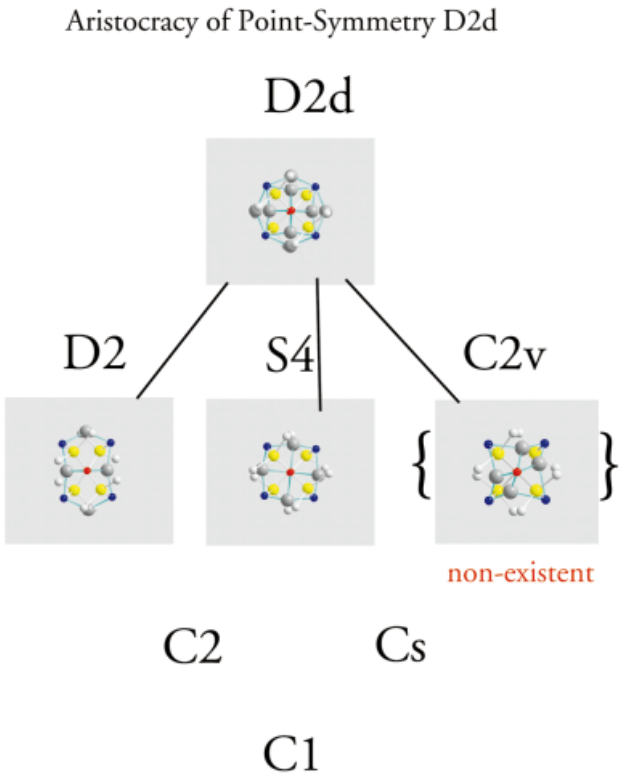

Figure 19. Symmetry tree of D_{2d}, S_4, and D_2; the sketch for C_{2v} is drawn for completeness but is not relevant

solid-state phase transitions have been found for $\mathbf{Li_4X_2}$. It is interesting to note that all structures determined within the $\mathbf{Li_4X_2}$ system or any other ligand derived from $[R-N-SiR'R''-O-SiR'R''-N-R]^{2-}$ can be classified within the $D_{2d}(\bar{4}2m)$ symmetry tree, as exemplified in Figure 19. From all point symmetries collected in Figure 19 only C_{2v} and C_s have not been realised in a crystalline compound, which is comprehensible because of the special arrangement of the two anionic ligands and the ionic repulsions of the four formal cations. As a matter of fact, all low-temperature structures can be classified to belong exactly or approximately to either D_2 or S_4 subgroup.

The second-order phase transition within $\mathbf{Li_4X_2}$ from space group $P4_2/n$ to $P4_2/nmc$ shows nicely that the amplitudes of the metal oscillations are temperature-dependent, and furthermore that ligand librations are involved in the whole process.

The replacement of lithium by sodium to form $\mathbf{Na_4X_2}$ parallels our findings within the O−Si−N−Si−O skeleton. Contrary to the lithium derivative $\mathbf{Li_4X_2}$ there are no important sodium oscillations. The phase transition from the orthorhombic to the tetragonal phase is again driven by entropy: In the high-temperature tetragonal phase all *tert*-butyl groups rotate around the N−C bonds, while in the low-temperature phase they are at rest. Only at the transition point do the sodium atoms show important displacements, but neither before nor after this transition point do the sodium atoms seem to be involved in important movements. The molecular point symmetry of $\mathbf{Na_4X_2}$ passes from approximately D_2 to S_4 at the transition, which means that in the transition state the D_{2d} symmetry has to be run through (Figure 19).

The *tert*-butyl/trimethylsilyl exchange on the nitrogen atoms in the lithium and sodium compounds enhances the ionic charge on nitrogen, and leads to a parallel effect with respect to the stability of structures. The structures found at room temperature with trimethylsilyl substituents and a N−Si−O−Si−N backbone can be only "copied" using *tert*-butyl in place of trimethylsilyl, if the temperature is maintained below ca. 250 K. Again, this corresponds with our findings in the O−Si−N−Si−O series.

The bulkiness of the ligands can influence the structure to such a point that no dimer can be formed any more (see $[t\mathrm{BuN}-\mathrm{Si}(i\mathrm{Pr})_2-\mathrm{O}-\mathrm{Si}(i\mathrm{Pr})_2-\mathrm{N}t\mathrm{Bu}]\mathrm{Li}_2$). The lithium/potassium derivative $\mathbf{Li_2K_2X_2}$ adopts the D_2 symmetry allowing different ligations to lithium and potassium atoms. The copper and silver derivatives $\mathbf{Cu_4X_2}$ and $\mathbf{Ag_4X_2}$ show almost linear N−M−N arrangements and no tendency to metal oscillations in accord with metal−nitrogen bonding different from that of lithium or sodium.

Metal motions in crystalline solids in distinct regions (metal movements in molecular boxes) merit increasing interest because they are anisotropic (in the cases discussed in this article the rotations or oscillations are perpendicular to the tetragonal [001] axis) and can be influenced. The simple switching on and off of these dynamics could lead to applications in solid-state physics. Instead of heat energy, a magnetic or electric field could also be used in principle.

Acknowledgments

I would like to thank S. Wieczorek, Dr. K. Fries, and Dr. J. Böhnlein-Maus for their synthetic work, Dr. V. Huch for the X-ray experiments, as well as Dr. M. Zimmer for solid-state NMR experiments. Prof. J. Krüger, Experimentalphysik, Saarbrücken, is acknowledged for the DSC curve of $\mathbf{Li_4X_2}$. With deep regret I have learnt of the sudden death of Prof. H. G. Unruh, Experimentalphysik, Saarbrücken, who conducted the single-crystal Raman experiments: I still remember well our fruitful discussions on phase transitions. This work has been financed partly by the Deutsche Forschungsgemeinschaft as well as the Fonds der Chemischen Industrie, which are acknowledged. I thank Dr. V. Subramanian for reading the manuscript.

[1] M. Veith, M. Zimmer, *Main Group Chem. News* **1994**, *2*, 12−16.
[2] M. Veith, M. Zimmer, P. Kosse, *Chem. Ber.***1994**, *127*, 2099−2102.
[3] M. Veith, M. Zimmer, *Z. Anorg. Allg. Chem.* **1996**, *622* 1471−1477.
[4] M. F. Lappert, P. P. Power, A. R. Sanger, R. C. Srivastava, *Metal and Metalloid Amides,* Ellis Horwood, New York − Chichester − Brisbane − Toronto, **1980**.
[5] M. Veith, M. Zimmer, S. Müller-Becker, *Angew. Chem.* **1993**, *105*, 1771−1773; *Angew. Chem. Int. Ed. Engl.* **1993**, *32*, 1731−1733.
[6] F. Maseras, A. Lledos, *J. Chem. Soc., Chem. Commun.* **1995**, 443−444.
[7] A. Sekiguchi, T. Matsuo, H. Sakurai, *Angew. Chem.* **1998**, *110*, 1752−1754; *Angew. Chem. Int. Ed.* **1998**, *37*, 1662−1664; Addition and Corrections: *Angew. Chem.* **1998**, *110*, 2569; *Angew. Chem. Int. Ed.* **1998**, *37*, 2292.
[8] A. J. Elias, H. W. Roesky, W. T. Robinson, G. M. Sheldrick, *J. Chem. Soc., Dalton Trans.* **1993**, 495−500.

[9] A. J. Elias, H. G. Schmidt, M. Noltemeyer, H. W. Roesky, *Eur. J. Solid State Inorg. Chem.* **1992**, *29 (Suppl.)*, 23−42.
[10] U. Wannagat, J. Herzig, P. Schmidt, M. Schulze, *Monatsh. Chem.* **1971**, *102*, 1817−1824.
[11] G. I. Harris, *J. Chem. Soc. B* **1970**, 488−500.
[12] L. Lochmann, J. Pospisil, D. Lim, *Tetrahedron Lett.* **1966**, *2*, 257−262.
[13] R. Pi, W. Bauer, B. Brix, C. Schade, P. von Ragué Scheyer, *J. Organomet. Chem.* **1986**, *306*, C1−C4.
[14] L. Lochmann, H. Jakubuv, L. Brandsma, *Collect. Czech. Chem. Commun.* **1993**, *58*, 1445−1451.
[15] M. Veith, M. Zimmer, K. Fries, J. Böhnlein-Maus, V. Huch, *Angew. Chem.* **1996**, *108*, 1647−1651; *Angew. Chem. Int. Ed. Engl.* **1996**, *35*, 1529−1533.
[16] M. Veith, A. Koban, K. Fries, P. Spaniol, R. Elsäßer, A. Rammo, V. Huch, U. Kleinsteuber, *Organometallics* **1998**, *17*, 2612−2618.
[17] M. Veith, S. Wieczorek, K. Fries, V. Huch, *Z. Anorg. Allg. Chem.* **2000**, *626*, 1237−1245.
[18] K. Fries, Dissertation, Saarbrücken, **1996**.
[19] M. Veith, S. Wieczorek, M. Zimmer, V. Huch, unpublished results.
[20] *HYPERCHEM 4.0*, Autodesk, Inc. USA **1996**. Parameters modified for Si and N by M. Veith.
[21] A. I. Kitaigorodskii, *Molecular Solids and Crystals*, Academic Press, New York, **1973**.
[22] H. G. Unruh, M. Veith, unpublished results.
[23] A. F. Hollemann, E. Wiberg, N. Wiberg, *Lehrbuch der anorganischen Chemie*, 101st ed., Walter de Gruyter, Berlin−New York, **1995**.
[24] M. Veith, *Z. Anorg. Allg. Chem.* **1978**, *446*, 227−236.
[25] R. E. Mulvey, *Chem. Soc. Rev.* **1991**, *20*, 167−209.
[26] J. Krüger, University of the Saarland, Physics Department, **1999**.
[27] N. G. Parsonage, L. A. K. Staveley, *Disorder in Crystals*, Clarendon Press, Oxford, **1978**, p. 1−45.
[28] J. H. Kristensen, H. Bildsoe, H. J. Jakobsen, N. C. Nielsen, *J. Magn. Reson*. **1992**, *100*, 437−443.
[29] L. E. Orgel, *J. Chem. Soc.* **1958**, 4186−4190.

Received November 15, 1999
[I99407]